Supplement of The Cryosphere Discuss., 9, 1503–1554, 2015
http://www.the-cryosphere-discuss.net/9/1503/2015/
doi:10.5194/tcd-9-1503-2015-supplement

The Cryosphere Discussions
Open Access

Supplement of

A macroscale mixture theory analysis of deposition and sublimation rates during heat and mass transfer in snow

A. C. Hansen and W. E. Foslien

Correspondence to: A. C. Hansen (hansen@uwyo.edu)

Foslien, Wayne E., A Modern Mixture Theory Applied to Heat and Mass Transfer in Snow, M.S., Department of Mechanical Engineering, July, 1994.

A modern mixture theory is applied to heat and mass transfer in snow to set the groundwork for a theory that can describe the microstructural evolution of snow. Two ideal microstructures are considered that represent the extremes in possible microstructures for snow. An effective thermal conductivity based on a linear combination of these two microstructures is then used in the energy equation. Numerical results are presented for the cases of a fluctuating boundary condition and a dense layer contained in the snowpack.

A MODERN MIXTURE THEORY APPLIED TO HEAT AND MASS TRANSFER IN SNOW

by
Wayne E. Foslien

A thesis submitted to the
Department of Mechanical Engineering and
the Graduate School of the University of Wyoming
in partial fulfillment of requirements
for the degree of

MASTER OF SCIENCE
in
MECHANICAL ENGINEERING

Laramie, Wyoming
July, 1994

TO THE OFFICE OF THE GRADUATE SCHOOL:

The members of the committee approve the thesis of Wayne E. Foslien presented on July 19, 1994.

_____

Andrew C. Hansen, Chairman

_____

William R. Lindberg

_____

Carl R. Reid

_____

Thomas V. Edgar

APPROVED:

_____

Kynric M. Pell, Head, Department of Mechanical Engineering

_____

Thomas G. Dunn, Dean of The Graduate School

ACKNOWLEDGEMENTS

The author wishes to express sincere appreciation to Dr. Andrew Hansen for his support and insightful discussions concerning the material presented here. Also I sincerely appreciate the financial support of the National Science Foundation and the Department of Energy.

TABLE OF CONTENTS

LIST OF TABLES

Page

LIST OF FIGURES

LIST OF SYMBOLS USED

ARABIC LETTERS

a	Acceleration ($m \cdot s^{-2}$)
A	Avogadro's number
b	Body force density ($N \cdot kg^{-3}$)
B	Body of continuous mixture
$\hat{c}$	Mass supply ($kg \cdot m^{-3} \cdot s^{-1}$)
C	Specific heat ($J \cdot kg^{-1} \cdot K^{-1}$)
D	Binary diffusion coefficient ($m^2 \cdot s^{-1}$)
$\hat{e}$	Energy supply ($W \cdot m^{-3}$)
F	Deformation gradient (dimensionless)
g	Acceleration due to gravity ($m \cdot s^{-2}$)
h	Time step (s)
H	Height of snowpack (m)
j	Diffusive flux ($kg \cdot m^{-2} \cdot s^{-1}$)
k	Thermal conductivity ($W \cdot m^{-1} \cdot K^{-1}$)
L	Length in microstructure (m)
L	Velocity gradient tensor (s^{-1})

M Molecular weight ($g \cdot gmole^{-1}$)

n Normal vector

N Total entropy ($J \cdot K^{-1}$)

$\hat{\mathbf{p}}$ Momentum supply ($N \cdot m^{-3}$)

P Pressure (Pa)

q Energy flux vector ($W \cdot m^{-2}$)

r Energy generation ($W \cdot kg^{-1}$)

t Time (s)

t Partial stress traction vector (Pa)

$\mathbf{t}^*$ True stress traction vector (Pa)

T Cauchy stress tensor (Pa)

u Specific internal energy ($J \cdot kg^{-1}$)

v Velocity ($m \cdot s^{-1}$)

V Volume (m^3)

x Current coordinates (m)

X Reference coordinates (m)

GREEK SYMBOLS

β Thermal expansion coefficient of air (K^{-1})

χ Mapping from reference to current coordinates

ε Specific instantaneous energy ($J \cdot kg^{-1}$)

ϕ Volume fraction

γ True constituent mass density ($kg \cdot m^{-3}$)

η Specific entropy ($J \cdot kg^{-1} \cdot K^{-1}$)

κ Permeability of the porous medium (m^2)

λ Thermal diffusivity ($m^2 \cdot s^{-1}$)

μ Dynamic viscosity (Pa·s)

θ Temperature (K)

ρ Dispersed density ($kg \cdot m^{-3}$)

σ Condensation or evaporation coefficient

ξ Specific surface area (m^{-1})

ψ Specific Helmholtz free energy ($J \cdot kg^{-1}$)

Ω Boltzmann's constant ($J \cdot K^{-1} \cdot molecule^{-1}$)

Ψ Any scalar, vector, or tensor-valued function

OPERATORS

∇ Gradient operator

$\dot{\Psi}$ Material time derivative

SUBSCRIPTS

a Air component

α Constituent

c	Characteristic of microstructure
con	Conduction
ha	Humid air constituent
i	Ice constituent
ref	Reference
s	Snow
sg	Change from solid to gas
T	Total
v	Water vapor component
v-a	Water vapor diffusing through air
x	Current coordinates

SUPERSCRIPTS

lam	Lamellae microstructure
macro	Macroscale
micro	Microscale
P	Constant pressure
pore	Pore microstructure
ref	Reference
s	Snow
sat	Saturated water vapor in air

$\bar{V}$	Constant volume
*	Dimensionless scalar

CHAPTER I

INTRODUCTION

Snow covers a large portion of the earth's surface at any one time, so interaction by humans is inevitable. For example, recreational activities such as skiing and snowmobiling have allowed the exploration of the backcountry alpine environment. Although very pristine on the surface, the winter alpine environment contains many hidden dangers. For one, snow on the alpine slope can pose the threat of avalanche.

The stratigraphy and microstructure of the snowpack are indicators of how resistant a sloped snowpack is to avalanche release. The snowpack typically has layers of varying densities. High density snow layers form when wind carries dendritic snow crystals across the snow surface breaking them up into tiny fragments. The result is close packing of ice fragments and thus a dense snow layer. Melting and refreezing of the surface by solar radiation and burial by subsequent snowfall can also cause a dense icy layer in the snowpack. Less dense layers form when dendritic snow crystals are allowed to accumulate. Thus, the stratigraphy of a snowpack can be very complex due to different environmental conditions during and after deposition.

Besides being stratigraphically complex, snow on the ground is also a thermodynamically active substance because of its high specific surface area and its likelihood to change phase. The snow microstructure readily goes through several metamorphic processes including disintegration of dendritic crystals, sintering and

bonding of grains, complete crystallographic changes, and melting and refreezing due to imposed environmental conditions. All changes in some way affect the strength of the snowpack and its resistance to avalanche.

One impact that dense layers have on snowpacks was observed by Adams and Brown (1982). They measured a relative decreases in snow strength above and below a dense layer in a snowpack subjected to a temperature gradient. They attributed this phenomenon to enhanced microstructure changes due to the dense snow layer.

This thesis is concerned with modeling the heat and mass transfer in snow in order to better understand the metamorphosis of snow. The interactions of stratigraphy, crystalline changes, and environmental conditions pose a difficult analytical problem. The tool best suited for this analysis was chosen to be the modern continuum mixture theory of Hansen (1989, 1991).

This chapter explains some of the microstructural changes in snow critical to avalanches and describes the modern mixture theory and its appropriateness for application to analyzing snow. Finally, previous work in modeling snow is discussed, and the scope of the thesis is defined.

SNOW METAMORPHISM CLASSIFICATIONS

Microstructural changes in dry snow can be broken down into two categories. The first category involves the changes snow experiences in the absence of a large temperature gradient ($<10^{o}$ C/m). This has been called equi-temperature metamorphism

(Sommerfeld & LaChapelle, 1970). The second category involves the changes snow experiences when a large temperature gradient is present. This has been called temperature gradient metamorphism (TGM) (Sommerfeld & LaChapelle, 1970). This section will describe both separately.

The equi-temperature metamorphism process begins as soon as the dendritic ice crystals reach the ground. Figure 1.1 shows a dendritic snow crystal going through the equi-temperature metamorphism process. The dendritic ice crystal is in a thermodynamically unstable state as its surface energy is very large. In order to reduce the crystal's surface energy, water molecules diffuse through the air from areas of high vapor pressure (small radii) to areas of low vapor pressure (large and negative radii). The result is that dendritic crystals lose their delicate shape and form more rounded ice crystals.

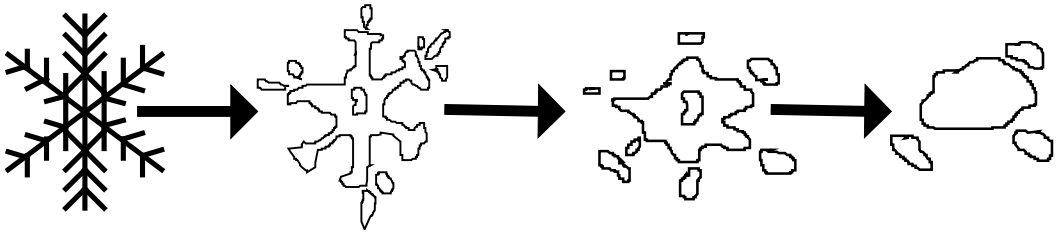

Figure 1.1. The Equi-Temperature Metamorphism Process of a Single Snow Crystal.

When equi-temperature grains are present, the snowpack is highly resistant to avalanche because most individual grains are joined by ice necks. The ice necks form when water vapor condenses at the junction of two touching crystals. The radius of curvature here is negative, and, therefore, the vapor pressure is much lower. This makes junctions between

ice crystals a likely place for water vapor to condense. When ice necks form, they tend to hold the snowpack together thereby increasing the snow's strength.

The process of temperature gradient metamorphism of snow is characterized by vapor transport through the snowpack due to an applied thermal gradient. A temperature gradient often exists in an alpine snowpack because the earth's thermal capacity keeps the snow near the ground close to freezing temperatures. The ambient air temperature readily fluctuates. Temperature gradient metamorphism proceeds most quickly when the air temperature drops significantly below zero thus establishing a temperature gradient in the snowpack. Because the amount of water vapor that the air can hold is a strong function of temperature, a water vapor density gradient also exists in the snowpack due to the temperature gradient. Water vapor diffuses from the warmer regions of the snowpack to colder regions. The water vapor diffusion causes growth of the depth hoar crystal. The term hoar refers to ice which forms from the vapor phase. The depth hoar crystal has the shape of a six-sided pyramid, and it has steps on each face which is characteristic of crystals undergoing rapid growth.

Figure 1.2 shows an idealized arrangement of growing depth hoar crystals with the average temperature profile and an actual temperature profile. Water vapor sublimes from the top of crystal I which is warmer than the average temperature of the snow at its height, diffuses through the air space, and condenses on the bottom of crystal II which is colder than the average snow temperature at its height. The top of crystal II also sublimes

and water vapor condenses on the bottom of crystal III. The depth hoar crystals often have rounded tops where sublimation is occurring and large bottoms where condensation is occurring. The water vapor diffuses on through the snowpack in this "hand-to-hand" fashion as first described by Yosida *et al.* (1955, in Colbeck, 1987).

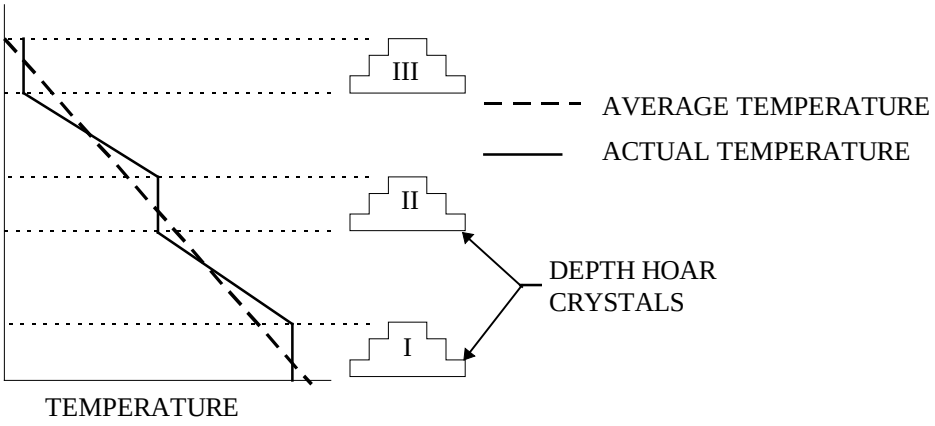

Figure 1.2. The Temperature Profile During Temperature Gradient Metamorphism (adapted from Sommerfeld & LaChapelle, 1970).

During active growth of depth hoar, the number of grain bonds decreases. Also the number of small rounded grains decreases as the size of the depth hoar increases. In other words, temperature gradient metamorphism can be such an active process of growth that hardly any original ice crystals survive. This includes any bonds that existed between ice grains. Temperature gradient metamorphism of snow with temperature gradients in excess of 10^{o} C/m dominate any radius of curvature effects that would produce bonding between grains. For example, Colbeck (1982) calculated that in a snowpack with a temperature gradient of 10^{o} C/m and ice grains with diameters of 10^{-2} cm, the temperature gradient is about 50 times more effective at moving vapor than the radius of curvature

differences. Therefore, temperature gradient metamorphism of snow results in a layer of segregated depth hoar crystals that is lower in strength. A layer of TGM snow can make an entire snowpack susceptible to avalanche.

OTHER MOTIVATIONS FOR STUDYING TGM

Besides the weakening effect that temperature gradient metamorphism has on the snowpack, another motivation for studying TGM is the degradation of load and shear bearing properties of snow runways and highways in the Arctic and Antarctic in the presence of a temperature gradient. The temperature gradient causes snow metamorphism which weakens layers in the snow. The lower strength properties translate into vehicle sinkage and traction loss.

Snow can also serve as a model of other important engineering processes such as powder metallurgy where solid, liquid, and vapor phases can all be present at once. Snow often exists near its melting point, so the possibility of phase change is very high. Furthermore, heat and mass flux through a snow layer are additional processes occurring simultaneously with phase change. These thermodynamic processes change the snow's grain shape, density, strength, permeability, and thermal properties.

Last of all, mass transfer in the snowpack is useful to study because pollutants redistribute themselves in the snow leading to the acid-pulse runoff phenomenon which has adverse effects on fragile ecosystems.

MIXTURE THEORY

The success of single continuum theories in modeling physical problems of solid mechanics, fluid flow, and heat transfer is widespread. All materials, however, when viewed on a small enough scale are neither homogeneous nor continuous. Most materials of interest are composed of several constituents each having their own physical and mechanical properties. For example, air is composed of nitrogen, oxygen, carbon dioxide, and other trace gases. Only the bulk properties of the mixture are necessary to model the flow of air. Hence, a single continuum theory is adequate to describe most problems of physical interest. Many other materials of physical interest such as composite materials, porous media, bubbly liquids, and snow can contain interactions amongst their constituents which are unaccounted for in a single continuum theory. The interactions between the constituents in these materials often require a more comprehensive treatment.

The idea of a continuum mixture must then be developed here in order that a theory can be developed to describe such a material. A continuum mixture is based on the definitions of a continuum and a mixture. The mixture is defined as a medium in which two or more materials or constituents are intermixed. Each constituent of the mixture is characterized by its own material properties. Furthermore, the continuum point is defined as a geometric point in space conceived as occupying no volume, but which retains properties associated with a finite volume by taking mathematical limits. Combining these two definitions results in the concept of a continuum mixture, which is

that a mixture continuum point contains all constituents present in the mixture and that each continuum mixture point retains the properties of each constituent present. The amount of each constituent present, denoted by the volume fraction, the interaction between constituents, and the other typical properties such as density, velocity, and temperature of each constituent are the variables of interest when developing the balance laws of a continuum mixture. The microstructure must be considered when developing the interactions between constituents.

Truesdell (1984) was the first person credited with formulating the balance equations for a continuum mixture of miscible components. This was termed the classical theory of mixtures. A miscible mixture is one in which its components can only be distinguished on the molecular scale. One miscible mixture is air, a mixture of ideal gases. The classical theory of mixtures has been slow to develop in its application to real physical problems (Bedford & Drumheller, 1983). Truesdell's work, however, spawned the interest in mixtures. Many theories since then have been developed to account for immiscible constituents. These theories have been called theories of materials with microstructure and volume fraction theories. These too have had little success in their application to real physical problems. Bedford and Drumheller (1983) review the development of many of these theories.

Recently the classical theory of mixtures has been shown to be in disagreement with the kinetic theory of gases in that it incorrectly predicts the pressure in a mixture of

ideal gases (Hansen, 1991). Hansen expresses his revisions to one "metaphysical" principle of Truesdell's (1984). Truesdell said that the motion of the mixture should be governed by the same equations as that of a single body. Hansen revised this "metaphysical" principle to say:

> The motion of the mixture is governed by the sum of the constituent balance equations. Furthermore, the equations of a single continuum must be recovered as a special case of the mixture relations.

Hansen (1989, 1991) has also formulated a volume fraction-based mixture theory based on the revised "metaphysical" principle. His theory correctly predicts the pressure in an ideal gas mixture as being the sum of the partial pressures of each constituent gas. His theory has also been successfully applied to the mechanics of composite materials (Hansen, 1994).

PREVIOUS WORK

Previous studies on temperature gradient metamorphism of snow can be classified into the areas of experimental and theoretical.

EXPERIMENTAL WORK. Bradley et al. (1977) studied temperature gradient metamorphism of snow in the natural setting of Yellowstone National Park. They distinguished three levels of depth hoar development: a fine-grained anhedral depth hoar, a subhedral depth hoar, and a fully-developed euhedral depth hoar. The anhedral depth hoar is a solid ice crystal having flat surfaces and sharp corners. The anhedral crystals are typically no longer than 1 mm. The subhedral depth hoar crystals are slightly larger with

lengths between 1 and 2 mm with some hollow construction. The euhedral depth hoar crystals are large, fully-developed hollow crystals. They found that of the three types of depth hoar, the layer which contained the subhedral depth hoar crystal corresponded to the weakest layer in the snowpack. This layer was found to be only 10 percent of its original strength. Temperature profiles also revealed that the largest temperature gradient in the snowpack occurred in the weakest layer in the snowpack. This would suggest that the thermal conductivity of the snow was a strong function of microstructure. However, their laboratory studies in which the boundary conditions were held constant could not confirm the large temperature gradient in the weak layer. The large temperature gradient could then have been due to the daily changes in temperature and solar radiation. Their laboratory studies did show a nonlinear profile at steady state with the largest temperature gradient occurring closest to the bottom where temperature gradient metamorphism had advanced the most. This does suggest that the thermal conductivity is definitely a function of microstructure. Because depth hoar crystals grow at the expense of the grain bonds, heat flow is impeded because air has a thermal conductivity about 100 times less than that of ice. Fourier's law of heat conduction says that the heat flux is proportional to the thermal conductivity times the temperature gradient. In order to maintain the heat flux, the temperature gradient increases in TGM snow because its thermal conductivity is reduced by the loss of grain bonds.

Adams and Brown (1982) verified the large temperature gradient in the weak layer in the laboratory in the absence of any fluctuations of surface temperature. This strengthens the idea that the microstructure strongly affects the thermal conductivity of the snow. Adams and Brown also conducted experiments in the lab with dense layers present in the experimental snowpack. They observed depth hoar growth and corresponding weakness below the dense layers. They attribute the depth hoar growth to a local increase in temperature gradient below the dense layer due to higher thermal conductivity of the dense layer. They claim that the dense layer conducts heat better. Therefore, the temperature gradient must be locally higher just above and below the dense layer.

In 1980, Marbouty conducted experiments to determine crystal size changes as a function of temperature, temperature gradient, density, and original crystal type. He then used this information in a numerical code which predicted the temperature in a snowpack in order to model the evolution of a snowpack in the presence of a temperature gradient. His results showed good agreement for a case not far from his experimental conditions used to determine the functional form of crystal size. A more elaborate model should include coupling between the microstructure evolution and such things as thermal conductivity and diffusion coefficient.

THEORETICAL WORK. The theoretical works on temperature gradient metamorphism of snow are divided into theories that predict microstructure evolution and

those that predict the heat and mass transfer in a snowpack. Rarely have the macroscopic and microscopic theories been included in one complete analysis of snow.

Colbeck (1983) used the potential field theory solutions of simple particle geometries to develop a model of depth hoar crystal growth as a function of temperature, temperature gradient, and condensation rate. He showed that depth hoar crystals are likely to grow below dense crust layers in the snowpack. He does not compare his microstructure model to experimental growth rates. Because Colbeck's model is based on the local temperature and temperature gradient in the snowpack, it is readily incorporated as a model for crystal growth rate into macroscopic theories.

Gubler (1985) improved Colbeck's microstructure model by applying the electrostatic analogy to clusters of particles. He also accounts for radius of curvature effects which are important at low temperature gradients.

Christon (1990) did the most in-depth numerical study of temperature gradient metamorphism of snow. He quantified the often disputed diffusion and heat transfer enhancement with his three-dimensional ice crystal model. He showed that the degree of enhancement of the diffusion coefficient depends on the ice crystal geometry and bracketed the range of experimental results with his numerical results. Christon was also able to show that the branch grains in his idealized microstructure geometry grow with flared bottoms much like the shape of depth hoar crystals. However, he did not include

densities of snow above 500 kg/m^3 which limits the use of his results in a layered snow cover where densities could easily exceed 500 kg/m^3.

Adams and Brown (1989, 1990) used a mixture theory to model the heat and mass transfer in snow. The mixture theory used is based on the mixture theory of Passman et al. (1984). In addition to the problems exposed by Hansen (1991), the mixture theory of Passman et al. (1984) contains several terms which are difficult to motivate physically.

SCOPE OF RESEARCH

The problem at hand here is to develop a model of temperature gradient metamorphism of snow that is based on the modern mixture theory of Hansen (1989, 1991). This mixture theory has had success in modeling the mechanics of composite materials (Hansen, 1994). Now this mixture theory is to be applied to a heat and mass transfer problem in order to broaden its range of applicability. In addition, the purpose of the model is to provide a stepping stone to a comprehensive treatment of temperature gradient metamorphism of snow involving microstructural changes, complete interactions with environment, and stratigraphic effects in the snow.

A numerical solution to the resulting mixture theory model is to be employed. The numerical solution will have flexibility for additions of complexities associated with the modeling of snow. The numerical model presented will calculate the effects due to a dense layer of snow in the snowpack. The numerical model also will calculate the net condensation rate of the vapor which is believed to enhance depth hoar crystal growth

(Colbeck, 1983). Furthermore, it will handle fluctuating temperature boundary conditions as an attempt to model the daily variations in ambient temperature. Finally, a comparison between the numerical results and the quantitative and qualitative experimental results of previous work will be included.

OVERVIEW

Chapter 2 begins with explaining the kinematics of the modern mixture theory used to model the heat and mass transfer in snow. The global balance equations are presented and reduced to local form. The balance equations are then applied to the heat and mass transfer in snow. Two ideal microstructures of snow are considered and their effective thermal conductivities are derived.

Chapter 3 includes a comparison of the effective thermal conductivities derived in Chapter 2 to experimental thermal conductivities. Based on a stereological argument, an effective thermal conductivity is hypothesized that is a linear combination of the thermal conductivities of the ideal microstructures. This is shown to be in excellent agreement with experimental results.

Chapter 4 shows the development of the finite element method used to solve the partial differential equations governing the heat and mass transfer in snow. It ends with a description of the FORTRAN program used to implement the numerical solution.

Chapter 5 then shows the numerical results of two test cases and describes how they correlate with experimental observations.

Chapter 6 summarizes the problem of heat and mass transfer in snow. Recommendations are then made for further research on the microstructure evolution of snow.

CHAPTER II

THEORY

In this chapter the volume fraction based mixture theory is developed in three-dimensional Euclidean space. The kinematic relationships necessary to describe the motion of a mixture are presented. The balance laws are developed, and the second law of thermodynamics is also discussed. Finally, the balance laws are reduced to the equations governing heat and mass transfer in snow.

KINEMATICS

The kinematics of mixture theory is based on considering a body B consisting of N intermixed continua. Each constituent may be thought of as a body B_α, α=1,2,3, . . .,N.

The two descriptions of motion most common in continuum mechanics are the Lagrangian and Eulerian description. The Lagrangian description of motion relates the current configuration B_α (t) to the reference configuration B^{ref} as illustrated in Figure 2.1a. The mapping from reference coordinates $\mathbf{X}_\alpha$ to current coordinates $\mathbf{x}_\alpha$ for the Lagrangian description of motion is

$$\mathbf{x}_\alpha = \boldsymbol{\chi}_\alpha(\mathbf{X}_\alpha, t) \quad . \tag{2.1}$$

The velocity of constituent α in the Lagrangian description is

$$\mathbf{v}_\alpha = \frac{\partial \boldsymbol{\chi}_\alpha(\mathbf{X}_\alpha, t)}{\partial t} \quad , \tag{2.2}$$

and the acceleration is

$$\mathbf{a}_\alpha = \frac{\partial^2 \boldsymbol{\chi}_\alpha(\mathbf{X}_\alpha, t)}{\partial t^2} \quad . \tag{2.3}$$

The deformation gradient $\mathbf{F}_\alpha$ is defined as

$$\mathbf{F}_\alpha = \mathbf{x}_\alpha \overleftarrow{\nabla} \quad . \tag{2.4}$$

In the above equation, the operator $\overleftarrow{\nabla}$ refers to the gradient taken with respect to the reference coordinates.

If the mapping is one-to-one, then the inverse must exist and be of the form

$$\mathbf{X}_\alpha = \boldsymbol{\chi}^{-1}(\mathbf{x}_\alpha, t) \quad . \tag{2.5}$$

Equation (2.5) is the mapping for the Eulerian description of body motion and is

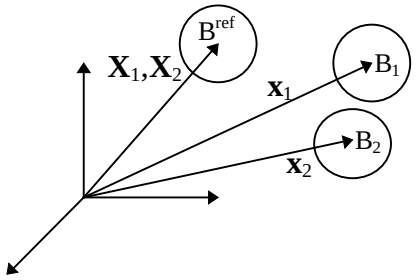

a) The Lagrangian Description

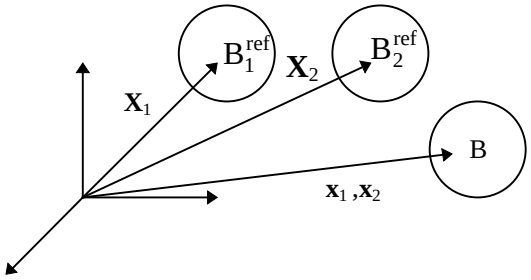

b) The Eulerian Description

Figure 2.1. Continuum Approaches for a Mixture of Constituents α, α=1,2.

illustrated in Figure 2.1b. In the Eulerian description, the independent variables are the current coordinates and time, and so the Eulerian description focuses attention on a given region of space. The Eulerian description is the most useful for fluid flow problems and will be used in this thesis to develop the balance laws and the second law of thermodynamics.

Because the current coordinates $\mathbf{x}_\alpha$ are a function of time, the chain rule is used to find the material time derivative of a function. The material time derivative in Eulerian coordinates of any scalar, vector, or tensor-valued function Ψ_α is

$$\dot{\Psi}_\alpha = \frac{\partial \Psi_\alpha}{\partial t} + (\Psi_\alpha \overleftarrow{\nabla}_x) \cdot \mathbf{v}_\alpha \quad . \tag{2.6}$$

The Eulerian description of motion often uses the velocity gradient which is defined as

$$\mathbf{L}_\alpha = \mathbf{v}_\alpha \overleftarrow{\nabla}_x \quad . \tag{2.7}$$

Here, the operator $\overleftarrow{\nabla}_x$ refers to the gradient taken with respect to the current coordinates. The deformation gradient and velocity gradient are related by

$$\dot{\mathbf{F}}_\alpha = \mathbf{L}_\alpha \cdot \mathbf{F}_\alpha \quad . \tag{2.8}$$

GENERAL PRINCIPLES

In this section, the basic physical laws of mass balance, momentum balance, and energy balance are developed for a continuum mixture. The second law of

thermodynamics is also presented. A more complete description of the balance law development can be found in Hansen (1989, 1991).

MASS BALANCE. The balance of mass equation for a constituent of a mixture can be developed by considering a fixed region R with boundary surface ∂R in body B. The balance of mass for constituent α in region R can be written as

$$\frac{\partial}{\partial t}\int_R \rho_\alpha dV = -\int_{\partial R} \rho_\alpha (\mathbf{v}_\alpha \cdot \mathbf{n}) dS + \int_R \hat{c}_\alpha dV \tag{2.9}$$

where ρ_α is the dispersed density, **n** is the unit normal to surface ∂R, and $\hat{c}_\alpha$ is the mass supplied to constituent α due to phase change or chemical reaction. The dispersed density is defined as

$$\rho_\alpha = \phi_\alpha \gamma_\alpha \tag{2.10}$$

where ϕ_α is the volume fraction of constituent α and γ_α is the true mass density of constituent α. In other words, γ_α is the mass of constituent α per unit volume of constituent α, whereas ρ_α is the mass of constituent α per unit volume of mixture. The volume fraction is necessary here because constituent α only occupies ϕ_α of volume R or covers ϕ_α of the entire surface ∂R. Quantitative stereology results have shown that the volume fraction is the same as the area fraction in a randomly distributed mixture (Underwood, 1970). The sum of the constituent volume fractions can be expressed as

$$\sum_\alpha \phi_\alpha = 1 \qquad . \tag{2.11}$$

An important constraint on the mass supply $\hat{c}_\alpha$ due to the fact that mass is neither created nor destroyed in the mixture is

$$\sum_\alpha \hat{c}_\alpha = 0 \quad . \tag{2.12}$$

For example, in a two constituent mixture composed of constituents α and β, the rate that constituent α changes to constituent β is equal and opposite to the rate at which constituent β is turning to constituent α.

Physically, equation (2.9) states that the rate of change of mass of constituent α in mixture volume R is due to two sources:

1) the flux of mass α across surface ∂R, and

2) the rate of mass supply to constituent α from other constituents due to chemical reactions or phase changes.

Upon applying the divergence theorem to the surface integral and noting that region R is fixed, equation (2.9) becomes

$$\int_R \left(\frac{\partial \rho_\alpha}{\partial t} + (\rho_\alpha \mathbf{v}_\alpha) \cdot \overleftarrow{\nabla}_x - \hat{c}_\alpha\right) dV = 0 \quad . \tag{2.13}$$

Because region R is arbitrary, the integrand must be zero. Equation (2.13) can then be written as

$$\frac{\partial \rho_\alpha}{\partial t} + (\rho_\alpha \mathbf{v}_\alpha) \cdot \overleftarrow{\nabla}_x = \hat{c}_\alpha \, . \tag{2.14}$$

which holds for each point in body B.

LINEAR MOMENTUM BALANCE. The balance of linear momentum for a constituent of the mixture is developed by again considering a region R with boundary ∂R in body B. The statement of balance of linear momentum for constituent α in region R is

$$\frac{\partial}{\partial t}\int_R \rho_\alpha \mathbf{v}_\alpha dV = -\int_{\partial R} \rho_\alpha \mathbf{v}_\alpha (\mathbf{v}_\alpha \cdot \mathbf{n}) dS + \int_{\partial R} \mathbf{t}_\alpha^{(\mathbf{n})} dS + \int_R (\rho_\alpha \mathbf{b}_\alpha + \hat{c}_\alpha \mathbf{v}_\alpha + \hat{\mathbf{p}}_\alpha) dV \qquad (2.15)$$

where $\mathbf{t}_\alpha^{(\mathbf{n})}$ is the partial stress traction acting on surface ∂R, $\mathbf{b}_\alpha$ is the body force density acting on constituent α, and $\hat{\mathbf{p}}_\alpha$ is the momentum supplied to constituent α due to interactions with other constituents. The partial stress traction can be written as

$$\mathbf{t}_\alpha^{(\mathbf{n})} = \phi_\alpha \mathbf{t}_\alpha^* \qquad (2.16)$$

where $\mathbf{t}_\alpha^*$ is the true stress traction on constituent α. Newton's third law of motion requires that

$$\sum_\alpha \hat{\mathbf{p}}_\alpha = \mathbf{0} \qquad . \qquad (2.17)$$

Physically, equation (2.15) states that the time rate of change of linear momentum inside region R is due to five sources:

1) the net flux of momentum across surface ∂R,

2) the partial stress traction $\mathbf{t}_\alpha^{(\mathbf{n})}$ acting on constituent α,

3) the body force acting on constituent α,

4) the rate of momentum gain due to mass gain of constituent α, and

5) the momentum supply $\hat{\mathbf{p}}_\alpha$ acting on constituent α due to interactions

with other constituents.

The partial stress tensor $\mathbf{T}_\alpha$ is defined as

$$\mathbf{t}_\alpha^{(\mathbf{n})} = \mathbf{n} \cdot \mathbf{T}_\alpha \quad . \tag{2.18}$$

After substituting equation (2.18) into equation (2.15), applying the divergence theorem to the surface integrals, and noting that the region R is arbitrary, the local form of the balance of linear momentum becomes

$$\rho_\alpha \mathbf{a}_\alpha = \vec{\nabla}_x \cdot \mathbf{T}_\alpha + \rho_\alpha \mathbf{b}_\alpha + \hat{\mathbf{p}}_\alpha \quad . \tag{2.19}$$

FIRST LAW OF THERMODYNAMICS. The first law of thermodynamics for constituent α is developed by considering a fixed region R and accounting for all energy transfer across its boundaries ∂R and all energy generated inside R. The statement of the first law of thermodynamics for constituent α is

$$\begin{aligned} \frac{\partial}{\partial t}\int_R \rho_\alpha \varepsilon_\alpha dV = -\int_{\partial R} \rho_\alpha \varepsilon_\alpha (\mathbf{v}_\alpha \cdot \mathbf{n}) dS + \int_{\partial R} (\mathbf{t}_\alpha^{(\mathbf{n})} \cdot \mathbf{v}_\alpha - \mathbf{q}_\alpha \cdot \mathbf{n}) dS + \\ \int_R [\rho_\alpha \mathbf{b}_\alpha \cdot \mathbf{v}_\alpha + \rho_\alpha r_\alpha + \hat{\mathbf{p}}_\alpha \cdot \mathbf{v}_\alpha + \hat{e}_\alpha + \hat{c}_\alpha \varepsilon_\alpha] dV \end{aligned} \tag{2.20}$$

where ε_α is the specific instantaneous energy of constituent α, $\mathbf{q}_\alpha$ is the energy flux vector, r_α is the heat generation term, and $\hat{e}_\alpha$ is the energy supply due to energy exchange between constituents. The specific instantaneous energy of constituent α is defined as

$$\varepsilon_\alpha = u_\alpha + \tfrac{1}{2} \mathbf{v}_\alpha \cdot \mathbf{v}_\alpha \tag{2.21}$$

where u_α is the internal energy of constituent α. Because energy is neither created nor destroyed in the mixture, a restriction on the energy supply term is

$$\sum_{\alpha} \hat{e}_{\alpha} = 0 \quad . \tag{2.22}$$

Equation (2.20) states that the rate of change of energy of constituent α is due to nine sources:

1) the net flux of energy across the surface ∂R,

2) the power supplied by surface tractions,

3) the energy flux out of the control volume R,

4) the power generated by the body force,

5) the volumetric generation of heat due to chemical reactions or radiation penetration,

6) the power generated by other constituents acting on constituent α,

7) the energy gain due to energy transfer between constituents, and

8) the energy gain due to mass gain of constituent α.

By the usual arguments, the local form of equation (2.20) becomes

$$\rho_{\alpha} \dot{u}_{\alpha} = \mathrm{tr}(\mathbf{T}_{\alpha} \cdot \mathbf{L}_{\alpha}) + \rho_{\alpha} r_{\alpha} - \vec{\nabla}_{x} \cdot \mathbf{q}_{\alpha} + \hat{e}_{\alpha} \quad . \tag{2.23}$$

SECOND LAW OF THERMODYNAMICS. The second law of thermodynamics for a mixture is developed by assigning a temperature and entropy density to each constituent in an arbitrary, fixed region R. Then the total entropy for the fixed region R is given by

$$N = \int_{R} \sum_{\alpha} \rho_{\alpha} \eta_{\alpha} \, dV \quad . \tag{2.24}$$

The second law governing the positive internal entropy production for the region R is

$$\dot{N} \geq \int_{\partial R} \sum_{\alpha} \frac{\mathbf{q}_\alpha}{\theta_\alpha} \cdot \mathbf{n}\, dS + \int_R \sum_{\alpha} \frac{\rho_\alpha r_\alpha}{\theta_\alpha} dV \quad . \tag{2.25}$$

The time derivative of the total entropy N can be written as

$$\dot{N} = \int_R \frac{\partial}{\partial t} (\sum_{\alpha} \rho_\alpha \eta_\alpha) dV + \int_{\partial R} \sum_{\alpha} (\rho_\alpha \eta_\alpha \mathbf{v}_\alpha \cdot \mathbf{n}) dS \quad . \tag{2.26}$$

By the usual arguments, the local form of the entropy equation becomes

$$\sum_{\alpha} [\rho_\alpha \dot{\eta}_\alpha + \eta_\alpha \hat{c}_\alpha + \frac{1}{\theta_\alpha} (\vec{\nabla}_x \cdot \mathbf{q}_\alpha - \rho_\alpha r_\alpha) - \frac{1}{\theta_\alpha^2} \vec{\nabla}_x \theta_\alpha \cdot \mathbf{q}_\alpha] \geq 0 \quad . \tag{2.27}$$

When the energy equation (equation (2.23)) and the Helmholtz free energy given by

$$\psi_\alpha = u_\alpha + \eta_\alpha \theta_\alpha \tag{2.28}$$

are substituted in equation (2.27), a more convenient form of the second law results given by

$$\sum \frac{1}{\theta_\alpha} [-\rho_\alpha (\dot{\psi}_\alpha + \eta_\alpha \theta_\alpha) + \mathrm{tr}(\mathbf{T}_\alpha \cdot \mathbf{L}_\alpha) + \hat{e}_\alpha - \frac{1}{\theta_\alpha} \vec{\nabla}_x \theta_\alpha \cdot \mathbf{q}_\alpha + \eta_\alpha c_\alpha \theta_\alpha] \geq 0 \quad . \tag{2.29}$$

Equation (2.29) can be used to find constitutive restrictions on the stress, energy supply, heat flux, and mass supply terms.

CONSTITUENT BALANCE EQUATIONS

In this section, the governing equations for a mixture are applied to the two constituents in the snow, namely, the ice and the humid air. Unlike Adams and Brown (1989, 1990), this analysis will not consider the momentum equation for either phase as

convection is unlikely to occur, and the stress in the ice phase calculated by the ice momentum equation has little practical use at this point in the analysis. Further justification for this simplification will be presented in the subsections that follow.

The terminology for the ice and humid air constituents needs further clarification. The terms phase and constituent as they apply to the ice are used interchangeably because ice is one constituent of the mixture, and it is also one phase of water. The humid air constituent is assumed to be a mixture of ideal gases, namely, water vapor and air. Thus, the term component will be used to refer to the water vapor or air alone.

SNOW MICROSTRUCTURE. The snow's microstructure plays a fundamental role in developing the balance equations. The interactions between the constituents and some proportionality constants must be derived from knowledge of the snow's microstructure.

Snow is typically thought of as a mixture of moist air with a random distribution of ice grains which are interconnected and, therefore, self-supporting. However, for the purposes of this theoretical development, two ideal microstructures are considered. Figure 2.2a shows a simple microstructure for the snow with pores parallel to the temperature gradient. In this pore microstructure, energy is transferred in parallel through the snowpack. The energy fluxes for the ice and humid air constituents, $\mathbf{q}_i$ and $\mathbf{q}_{ha}$, are simply added together to obtain the total energy flux through the snowpack. The second microstructure considered in the analysis is shown in Figure 2.2b. In this microstructure,

energy flows in series through the humid air and ice constituents, i.e. the temperature gradient is perpendicular to the lamellae. Therefore, the energy flux in the humid air constituent must be equal to the energy flux in the ice constituent. These two microstructures which were first considered by de Quervain (1963) produce two very different heat and mass transfer results and are believed to represent the extremes in possible microstructures for the snow.

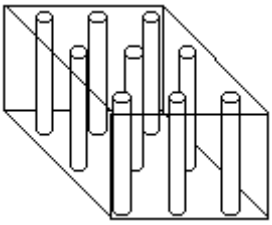

a) Pore Microstructure.

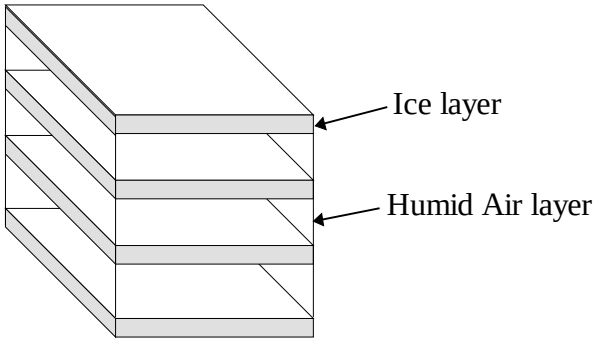

b) Lamellae Microstructure.

Figure 2.2. Ideal Snow Microstructures.

ICE CONSTITUENT MASS BALANCE. The balance of mass equation for the ice is

$$\frac{\partial \rho_i}{\partial t} + (\rho_i \mathbf{v}_i) \cdot \overleftarrow{\nabla}_x = \hat{c}_i \quad . \tag{2.30}$$

If the true mass density of the ice is constant and any settling velocity of the ice is neglected, the balance of mass equation for the ice becomes

$$\gamma_i \frac{\partial \phi_i}{\partial t} = \hat{c}_i \quad . \tag{2.31}$$

The above equation states that an increase in volume fraction of the ice constituent (increase in snow density) is only due to the phase change of water vapor to ice. This equation holds for either the pore or lamellae microstructure.

WATER VAPOR COMPONENT MASS BALANCE. Only the mass balance for the water vapor is considered here because the air acts only as the medium through which the water vapor diffuses.

For a porous material like snow and the pore microstructure of Figure 2.2a, Darcy's law states that the velocity of the humid air $\mathbf{v}_{ha}$ is proportion to the total pressure gradient. Darcy's law (Nield and Bejan, 1992) is

$$\mathbf{v}_{ha} = -\frac{\mu}{\kappa} \vec{\nabla}_x P_T \tag{2.32}$$

where μ is the viscosity of the humid air and κ is the permeability of the snow. For the lamellae microstructure, no bulk movement of the humid air can occur. For the pore microstructure, the motion of the vapor can be expressed as (Bird, 1960)

$$\gamma_v \mathbf{v}_v = \frac{\gamma_v}{\gamma_{ha}} (\gamma_a \mathbf{v}_a + \gamma_v \mathbf{v}_v) + \mathbf{j}_v \quad . \tag{2.33}$$

where the subscripts 'a' and 'v' refer to the air and water vapor components of the humid air, respectively. Equation (2.33) says that the mass flux of the water vapor is due to the bulk fluid motion of the air and water vapor mixture scaled by the mass fraction of water vapor in the humid air plus a relative velocity of the vapor due to diffusion. For the pore microstructure, equation (2.32) shows that when the total pressure in the humid air phase is uniform, the velocity of the humid air is zero. Therefore, for both microstructures, the barycentric velocity of the humid air can be expressed as (Bird, 1960)

$$\gamma_{ha}\mathbf{v}_{ha} = \gamma_v\mathbf{v}_v + \gamma_a\mathbf{v}_a = \mathbf{0} \quad . \tag{2.34}$$

This leaves for the pore microstructure

$$\gamma_v\mathbf{v}_v = \mathbf{j}_v = -\gamma_{ha}D_{v-a}\vec{\nabla}_x\left(\frac{\gamma_v}{\gamma_{ha}}\right) \tag{2.35}$$

from Fick's law of diffusion (Bird, 1960) where $D_{v\text{-}a}$ is the binary diffusion coefficient for water vapor in air. For the case of the lamellae microstructure, the mass flux is written as

$$\phi_v\gamma_v\mathbf{v}_v = \mathbf{j}_v = -\gamma_{ha}D_{v-a}\vec{\nabla}_x\left(\frac{\gamma_v}{\gamma_{ha}}\right) \tag{2.36}$$

because in the lamellae microstructure the diffusion velocity is enhanced since an ice layer acts simultaneously as a source and sink of water vapor. In other words, it takes the same amount of time for the water vapor to travel L_c, the characteristic length of the microstructure, as it does to travel the distance L_{ha}, the characteristic length of the humid air constituent at the microstructure level, through the humid air constituent. In equation form, this is

$$\frac{L_c}{\gamma_v \mathbf{v}_v} = \frac{L_{ha}}{\mathbf{j}_v} \quad . \tag{2.37}$$

or rearranging

$$\phi_v \gamma_v \mathbf{v}_v = \mathbf{j}_v \quad . \tag{2.38}$$

The volume fraction replaces the lineal fraction of the humid air constituent because stereological results state that the lineal fraction is equal to the volume fraction in a randomly distributed mixture. Because both water vapor and air occupy the entire pore space of the snow, the volume fraction of the water vapor is equal to the volume fraction of the humid air constituent or

$$\phi_v = \phi_{ha} = \phi_a \quad . \tag{2.39}$$

Therefore, all three volume fractions above may be used interchangeably in the balance equations.

The diffusive flux can be expanded to give

$$\mathbf{j}_v = -D_{v-a} \vec{\nabla}_x \gamma_v + \frac{\gamma_v}{\gamma_{ha}} D_{v-a} \vec{\nabla}_x \gamma_{ha} \quad , \tag{2.40}$$

but the second term on the right is negligibly small because the mass fraction of saturated water vapor in air at 273 K is about 4×10^{-3}.

The balance of mass for the vapor phase can be written as

$$\frac{\partial \rho_v}{\partial t} + (\rho_v \mathbf{v}_v) \cdot \vec{\nabla}_x = \hat{c}_v \quad . \tag{2.41}$$

Substitution of the diffusive flux into equation (2.41) gives

$$\frac{\partial \rho_v}{\partial t} - [\phi_v D_{v-a} \vec{\nabla}_x \gamma_v] \cdot \vec{\nabla}_x = \hat{c}_v \quad . \tag{2.42}$$

When equation (2.12) is expanded in terms of the mass supplies for the vapor and ice, it gives

$$\hat{c}_i + \hat{c}_v = 0 \quad . \tag{2.43}$$

Rearranging the above equation and defining the mass supply $\hat{c}$ to be positive when water vapor is condensing to form ice gives

$$\hat{c} = \hat{c}_i = -\hat{c}_v \quad . \tag{2.44}$$

Expanding the partial time derivative of the dispersed density of the water vapor gives

$$\frac{\partial \rho_v}{\partial t} = \gamma_v \frac{\partial \phi_v}{\partial t} + \phi_v \frac{\partial \gamma_v}{\partial t} \quad , \tag{2.45}$$

but from equation (2.11),

$$\frac{\partial \phi_i}{\partial t} = -\frac{\partial \phi_v}{\partial t} \quad . \tag{2.46}$$

Equations (2.45) and (2.46) along with the mass balance equation for the ice (equation (2.31)) can be used to simplify equation (2.42) to give

$$\phi_v \frac{\partial \gamma_v}{\partial t} - \vec{\nabla}_x \cdot (\phi_v D_{v-a} \vec{\nabla}_x \gamma_v) = \hat{c}\left(\frac{\gamma_v}{\gamma_i} - 1\right) \quad , \tag{2.47}$$

but the quantity $\frac{\gamma_v}{\gamma_i}$ is much less than one. Neglecting this term, the mass balance equation for the water vapor can then be written as

$$\phi_v \frac{\partial \gamma_v}{\partial t} = \vec{\nabla}_x \cdot (\phi_v D_{v-a} \vec{\nabla}_x \gamma_v) - \hat{c} \quad . \tag{2.48}$$

This equation holds for the pore microstructure but must be modified slightly for the lamellae microstructure because of the diffusive flux definition given by equation (2.38). The balance of mass equation for the lamellae structure is

$$\phi_v \frac{\partial \gamma_v}{\partial t} = \vec{\nabla}_x \cdot (D_{v-a} \vec{\nabla}_x \gamma_v) - \hat{c} \quad . \tag{2.49}$$

Equations (2.48) and (2.49) state that local changes in water vapor density are due to the divergence of vapor flux and sublimation. The temperature dependence of the diffusion coefficient is taken into account by noting that it is proportional to $\theta_{ha}^{\frac{3}{2}}$ (Incropera and DeWitt, 1985).

ICE CONSTITUENT MOMENTUM BALANCE. The momentum balance for the ice phase can be used to find the stress and strain in the ice phase of the snow. However, the effect that the ice stress has on the vapor density of the water is neglected in this analysis, so the ice phase momentum balance is not considered further.

HUMID AIR CONSTITUENT MOMENTUM BALANCE. The momentum balance for the humid air phase becomes important when bulk fluid motion occurs as in the case of convection or wind pumping. The Rayleigh number for a porous medium like snow is defined as (Nield and Bejan, 1992)

$$Ra = \frac{\gamma_{ha} g \beta \kappa H \Delta \theta}{\mu \lambda} \tag{2.50}$$

where g is the acceleration due to gravity, β is the thermal expansion coefficient of air, H is the height of the snowpack, and λ is the thermal diffusivity defined by

$$\lambda = \frac{k_s}{\gamma_a C_a^P} \tag{2.51}$$

where k_s is the thermal conductivity of the snow, γ_a is the density of the air, and C_a^P is the specific heat of air at constant pressure. With the values shown in Table 2.1, the Rayleigh number was calculated to be 0.2. The minimum critical Rayleigh number for the onset of convection in a snowpack is 9.87 (Nield and Bejan, 1992), so convection is unlikely to occur except in extreme circumstances. Therefore, the momentum balance for the humid air constituent was not considered further.

ICE CONSTITUENT ENERGY BALANCE FOR THE PORE MICROSTRUCTURE. The energy balance for the ice phase of a pore microstructure is

$$\rho_i \dot{u}_i = \mathrm{tr}(\mathbf{T}_i \cdot \mathbf{L}_i) + \rho_i r_i - \vec{\nabla}_x \cdot \mathbf{q}_i + \hat{e}_i \quad . \tag{2.52}$$

Table 2.1. Values used to calculate Rayleigh number.

γ_{ha}	$1.3 \frac{kg}{m^3}$
β	$3.7 \times 10^{-3}\ K^{-1}$
κ	$10^{-9}\ m^2$
H	1 m
$\Delta\theta$	40 K
μ	$1.72 \times 10^{-5}\ Pa \cdot s$
λ	$5.21 \times 10^{-4} \frac{m^2}{s}$

In this analysis, the ice phase is not moving and any work due to strain rates can be neglected. Also heat generation in the ice phase due to solar radiation is neglected. This

could easily be included as Colbeck (1989) and McComb *et al*. (1992) have done. These assumptions reduce equation (2.52) to

$$\rho_i \dot{u}_i = -\vec{\nabla}_x \cdot \mathbf{q}_i + \hat{e}_i \quad . \tag{2.53}$$

The internal energy for the nondeforming ice is assumed to be only a function of temperature and can be defined as

$$u_i = C_i^{\forall}(\theta_i - \theta_{ref}) + u_{i_{ref}} \tag{2.54}$$

where $C_i^{\forall}$ is the specific heat of ice at constant volume, and θ_{ref} is the temperature at the reference value of the internal energy $u_{i_{ref}}$. Without loss of generality, $u_{i_{ref}}$ can be set to zero. The heat flux is expressed by Fourier's law of heat conduction as

$$\mathbf{q}_i = -\phi_i k_i \vec{\nabla}_x \theta_i \quad . \tag{2.55}$$

Substitution of equations (2.54) and (2.55) into equation (2.53) gives

$$\phi_i \gamma_i C_i^{\forall} \frac{\partial \theta_i}{\partial t} = \vec{\nabla}_x \cdot (\phi_i k_i \vec{\nabla}_x \theta_i) + \hat{e}_i \quad . \tag{2.56}$$

Equation (2.56) is used to calculate the temperature in the ice phase and says that changes in temperature with time are due to the divergence of the heat flux in the ice phase and energy exchange between constituents.

HUMID AIR CONSTITUENT ENERGY BALANCE FOR THE PORE MICROSTRUCTURE. The energy balance for the humid air constituent in the pore microstructure is

$$\rho_{ha} \dot{u}_{ha} = \mathrm{tr}(\mathbf{T}_{ha} \cdot \mathbf{L}_{ha}) + \rho_{ha} r_{ha} - \vec{\nabla}_x \cdot \mathbf{q}_{ha} + \hat{e}_{ha} \quad . \tag{2.57}$$

As with the ice phase, the work term and energy generation term of the humid air constituent are neglected. The energy equation for the humid air constituent then reduces to

$$\rho_{ha}\dot{u}_{ha} = -\vec{\nabla}_x \cdot \mathbf{q}_{ha} + \hat{e}_{ha} \quad . \tag{2.58}$$

The definition of the internal energy for the humid air mixture of ideal gases is

$$\gamma_{ha}u_{ha} = \gamma_a u_a + \gamma_v u_v \tag{2.59}$$

or

$$\gamma_{ha}u_{ha} = \gamma_a[C_a^v(\theta_{ha} - \theta_{ref})] + \gamma_v[C_v^v(\theta_{ha} - \theta_{ref}) + u_{sg}] \tag{2.60}$$

where u_{sg} is the internal energy change when the water changes from a solid to a vapor. In equation (2.60), the reference value for the internal energy of the air has been set to zero without any loss of generality. In order to account for the fact that the internal energy of the water vapor is much higher than that of ice, the reference value of the internal energy for the water vapor has been set to the internal energy change when water changes from a solid to a vapor.

The definition of the energy flux vector for water vapor diffusing through air is (Bird, 1960)

$$\mathbf{q}_{ha} = -\phi_{ha}k_{ha}\vec{\nabla}_x\theta_{ha} - \phi_{ha}u_{sg}D_{v-a}\vec{\nabla}_x\gamma_v \quad . \tag{2.61}$$

The energy flux vector $\mathbf{q}_{ha}$ is composed of a conduction term and a term due to diffusion of water vapor carrying latent heat. The energy equation for the humid air constituent is found by first taking the material time derivative of the humid air constituent internal

energy defined in equation (2.60) which for constant specific heat, latent heat, humid air density γ_{ha}, and no humid air velocity gives

$$\dot{u}_{ha} = \frac{\gamma_a C_a^{\forall} + \gamma_v C_v^{\forall}}{\gamma_{ha}} \frac{\partial \theta_{ha}}{\partial t} + \frac{u_{sg}}{\gamma_{ha}} \frac{\partial \gamma_v}{\partial t} \quad . \tag{2.62}$$

Substitution of equations (2.61) and (2.62) into equation (2.58) gives

$$\begin{aligned} \phi_{ha} \left(\gamma C^{\forall} \right)_{ha} \frac{\partial \theta_{ha}}{\partial t} + u_{sg} \left(\phi_{ha} \frac{\partial \gamma_v}{\partial t} - \vec{\nabla} \cdot \left(\phi_{ha} D_{v-a} \vec{\nabla}_x \gamma_v \right) \right) \\ = \vec{\nabla}_x \cdot \left(\phi_{ha} k_{ha} \vec{\nabla}_x \theta_{ha} \right) + \hat{e}_{ha} \end{aligned} \tag{2.63}$$

where

$$\left(\gamma C^{\forall} \right)_{ha} = \gamma_a C_a^{\forall} + \gamma_v C_v^{\forall} \tag{2.64}$$

but

$$\hat{c} = \vec{\nabla}_x \cdot (\phi_v D_{v-a} \vec{\nabla}_x \gamma_v) - \phi_v \frac{\partial \gamma_v}{\partial t} \tag{2.65}$$

from the mass balance of the water vapor. Substituting equation (2.65) into equation (2.63) gives

$$\phi_{ha} \gamma_{ha} C_{ha}^{\forall} \frac{\partial \theta_{ha}}{\partial t} = \vec{\nabla}_x \cdot (\phi_{ha} k_{ha} \vec{\nabla}_x \theta_{ha}) + \hat{e}_{ha} + u_{sg} \hat{c} \quad . \tag{2.66}$$

The above equation is used to calculate the temperature in the humid air constituent of the snow with a pore microstructure. It says that changes in temperature of the humid air constituent with time are due to the divergence of the conductive energy flux in the humid air constituent, energy exchange between constituents, and latent heat release when water changes phase. Since the mass fraction of water vapor in saturated air is small at

temperatures below freezing, the density, specific heat, and thermal conductivity properties of humid air can be taken to be that of dry air. Also, for the sake of brevity, the subscripts for the volume fraction, temperature, and energy exchange of humid air are changed to the letter 'a' since the volume fraction, temperature, and energy exchange are the same for the air as for the humid air. The energy equation for the humid air constituent can then be written as

$$\phi_a \gamma_a C_a^{\forall} \frac{\partial \theta_a}{\partial t} = \vec{\nabla}_x \cdot (\phi_a k_a \vec{\nabla}_x \theta_a) + \hat{e}_a + u_{sg} \hat{c} \quad . \tag{2.67}$$

The latent heat term in equation (2.67) occurs in the energy equation for the humid air constituent because this constituent contains the diffusing water vapor which turns to ice at the air/ice interface. In reality, some of this latent heat will be conducted into the humid air constituent while some of it will be conducted into the ice. In fact, most of the latent heat will be conducted into the ice phase because the thermal conductivity is on the order of 100 times larger than that of air. In the sections that follow, this complication is resolved by discovering that the ice and humid air energy equations can be added together to obtain one energy equation for the snow.

ENERGY BALANCE FOR SNOW WITH LAMELLAE MICROSTRUCTURE.

In the case of the lamellae microstructure, one energy balance equation is written for the mixture of ice and humid air. The constituents are assumed to be at identical temperatures at a continuum point. The energy equation for the snow mixture is given by

$$\rho_i \dot{u}_i + \rho_{ha} \dot{u}_{ha} = -\vec{\nabla}_x \cdot \mathbf{q}_s \quad . \tag{2.68}$$

Following the development of the previous energy equations with the same internal energy definitions, the above equation becomes

$$(\phi_a \gamma_a \overline{C}_a^{v} + \phi_i \gamma_i \overline{C}_i^{v}) \frac{\partial \theta_s}{\partial t} = \vec{\nabla}_x \cdot [k_{con} \vec{\nabla}_x \theta_s] + \hat{c} u_{sg} \tag{2.69}$$

where θ_s is the temperature of the snow and k_{con} is the effective thermal conductivity of the snow due to conduction only.

The effective thermal conductivity of the snow is found by noting that the energy flux through the humid air constituent must be equal to the energy flux through the ice constituent. In equation form, this statement is

$$\mathbf{q}_s = -k_i \vec{\nabla}_i \theta_i = -k_{ha} \vec{\nabla}_{ha} \theta_{ha} - u_{sg} D_{v-a} \vec{\nabla}_{ha} \gamma_v \quad . \tag{2.70}$$

Here, the operator $\vec{\nabla}_\alpha$ refers to the gradient taken with respect to the differential length in the α constituent. At the microstructure level, the temperature gradients are allowed to be different in the two constituents in order to arrive at the correct effective thermal conductivity for the lamellae microstructure. When the vapor in the humid air constituent is saturated, equation (2.70) can be rewritten as

$$\mathbf{q}_s = -k_i \vec{\nabla}_i \theta_i = -k_{ha} \vec{\nabla}_{ha} \theta_{ha} - u_{sg} D_{v-a} \frac{d\gamma_v^{sat}}{d\theta} \vec{\nabla}_{ha} \theta_{ha} \quad . \tag{2.71}$$

The average temperature gradient in the snow can be expressed as

$$\vec{\nabla}_x \theta_s = \phi_i \vec{\nabla}_i \theta_i + \phi_{ha} \vec{\nabla}_{ha} \theta_{ha} \quad . \tag{2.72}$$

The heat flux through the snow can also be written as

$$\mathbf{q}_s = -k_{con} \vec{\nabla}_x \theta_s \quad . \tag{2.73}$$

Substitution of equations (2.71) and (2.72) into equation (2.73) gives

$$k_{con} = \frac{k_i k_{ha}}{\phi_i \left(k_{ha} + u_{sg} D_{v-a} \frac{d\gamma_v^{sat}}{d\theta} \right) + \phi_{ha} k_i} \quad . \tag{2.74}$$

When the mass supply for the lamellae microstructure defined by equation (2.49) is substituted for the mass supply in equation (2.69), an effective thermal conductivity which includes an enhancement due to diffusion can be calculated. This effective thermal conductivity is

$$k_{con+d}^{lam} = \frac{k_i \left(k_{ha} + u_{sg} D_{v-a} \frac{d\gamma_v^{sat}}{d\theta} \right)}{\phi_i \left(k_{ha} + u_{sg} D_{v-a} \frac{d\gamma_v^{sat}}{d\theta} \right) + \phi_{ha} k_i} \quad . \tag{2.75}$$

The thermal conductivity k_{con+d}^{lam} is the thermal conductivity that would be measured experimentally in a lamellae microstructure consisting of ice and humid air.

EVALUATION OF INTERACTION TERMS. The mass supply term $\hat{c}$ and the energy supply terms $\hat{e}_i$ and $\hat{e}_a$ need to be evaluated to close the system of equations for the snow. However, from equation (2.22) the energy supply terms are related by

$$\hat{e}_i = -\hat{e}_a \quad . \tag{2.76}$$

From equation (2.31), the physical interpretation for the mass supply term is the mass rate at which water vapor is condensing to form ice per unit volume of snow. Hobbs (1974) gave an expression for vapor condensation in terms of the vapor density difference

between the pore vapor density and the saturated vapor density over the ice. This expression is

$$\hat{c} = \frac{\sigma\xi R\theta_i^{1/2}(\gamma_v - \gamma_v^{sat})}{(2\pi\frac{M}{A}\Omega)^{\frac{1}{2}}}\frac{M}{A} \tag{2.77}$$

where σ is the condensation or evaporation coefficient, ξ is the specific surface area of the snow, R is the gas constant for water vapor, M is the molecular weight of water, A is Avogadro's number, and Ω is Boltzmann's constant. In the absence of diffusion, the mass balance equation for the water vapor can be written as

$$\phi_v\frac{\partial\gamma_v}{\partial t} = -\frac{\sigma\xi R\theta_i^{1/2}(\gamma_v - \gamma_v^{sat})}{(2\pi\frac{M}{A}\Omega)^{\frac{1}{2}}}\frac{M}{A} \quad . \tag{2.78}$$

If the saturated vapor density over the ice is held constant, the time for the vapor density difference between the pore density and the saturated density to become 0.1% of the initial density difference equilibrium can be calculated. This expression is given by

$$t = 6.91\cdot(1000\frac{g}{kg})^{\frac{1}{2}}\frac{\phi_v(2\pi\frac{M}{A}\Omega)^{\frac{1}{2}}}{\sigma\xi R\theta_i^{\frac{1}{2}}}\frac{A}{M} \quad . \tag{2.79}$$

A typical value of the specific surface area given by Hansen (1986) is 2430 m^2/m^3 for a snow density of 360 kg/m^3. The specific surface area was assumed to vary linearly with the ice volume fraction. For a snow density of 200 kg/m^3, the specific surface of the snow is 1400 m^2/m^3. Delaney *et al*. (1964) measured the condensation coefficient σ of ice to be 0.0144 for temperatures between -2 and -13 ^oC. With these values, the time for the vapor density in the pore to reach equilibrium is approximately $1.1x10^{-3}$ seconds.

Since the vapor density in the pore reaches equilibrium so quickly, the vapor density in the pore can be assumed to be the saturated vapor density throughout the process of metamorphism of snow.

A form for the energy supply terms that satisfies the second law of thermodynamics is

$$\hat{e}_{ha} = -\hat{e}_i = \hat{e}_o(\theta_i - \theta_{ha}) \quad . \tag{2.80}$$

The coefficient $\hat{e}_o$ is the constant of proportionality describing the rate at which the constituent temperatures reach equilibrium by conduction at the microstructure level. Two approaches are taken in order to determine how quickly the temperatures of the ice and humid air constituents come to equilibrium. The first approach is a time scale analysis comparing the time scale for heat transfer at the snowpack level to that at the microstructure level. The second approach actually approximates the coefficient $\hat{e}_o$ and then calculates a time for the constituents to come to thermal equilibrium.

The first approach starts by writing the single continuum equation describing one-dimensional heat conduction in each constituent. It is given by

$$\frac{\partial\theta}{\partial t} = \frac{k}{\gamma C}\frac{\partial^2\theta}{\partial x^2} \quad . \tag{2.81}$$

Equation (2.81) is nondimensionalized by defining the following nondimensional variables and substituting them into equation (2.81):

$$t^* = \frac{t}{t_o} \quad , \qquad x^* = \frac{x}{L_c} \quad , \qquad \theta^* = \frac{\theta - \theta_{init}}{\theta_f - \theta_{init}} \quad .$$

The resulting nondimensional equation is

$$\frac{\partial \theta^*}{\partial t^*} = \frac{t_o}{L_c^2}\frac{k}{\gamma C}\frac{\partial^2 \theta^*}{\partial x^{*2}} \quad . \tag{2.82}$$

The time scale t_o^{micro} for heat conduction on the microscale must then be

$$t_o^{micro} \approx \frac{\gamma C L_c^2}{k} \quad . \tag{2.83}$$

The time scale t_o^{macro} for heat conduction in a snowpack is defined similarly as

$$t_o^{macro} \approx \frac{\left(\phi_i \gamma_i C_i^{\forall} + \phi_a \gamma_a C_a^{\forall}\right) H^2}{\phi_i k_i + \phi_a k_a} \tag{2.84}$$

where H is the height of the snowpack which is much greater than the characteristic length of the microstructure. The ratio of the time scale for heat conduction in a snowpack to the time scale for heat conduction on the microscale for a snowpack density of 200 kg/m^3, a depth of 1 m deep, and a microscale characteristic length of 1 mm (Christon, 1990) is a minimum of 9×10^5 which suggests that thermal equilibrium between the ice and humid air constituents is a good assumption.

The coefficient $\hat{e}_o$ was estimated by considering a simple conduction model for the pore microstructure as shown in Figure 2.3. The Figure 2.3 shows the electrical analogy to heat conduction at the microstructure level. The coefficient $\hat{e}_o$ is given by

$$\hat{e}_o = \frac{\xi}{[L_c(\frac{\phi_a}{k_a} + \frac{\phi_i}{k_i})]} \tag{2.85}$$

where ξ is the specific surface area of the snow and is included here to convert units of $\hat{e}_\alpha$ to watts per m^3 of snow.

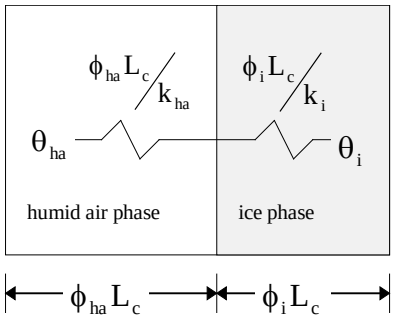

Figure 2.3. Simple Heat Conduction Model for Heat Transfer at the Snow Microstructure Level.

This model assumes that the temperature profile in each constituent is always linear. The heat conduction equations for the ice phase and the vapor phase assuming no heat conduction into the microstructure volume and no condensation is occurring can then be written as

$$\phi_{ha} \gamma_{ha} C_{ha}^{\forall} \frac{\partial \theta_{ha}}{\partial t} = \frac{\xi}{[L_c (\frac{\phi_a}{k_a} + \frac{\phi_i}{k_i})]} (\theta_i - \theta_{ha}) \tag{2.86}$$

and

$$\phi_i \gamma_i C_i^{\forall} \frac{\partial \theta_i}{\partial t} = \frac{\xi}{[L_c (\frac{\phi_a}{k_a} + \frac{\phi_i}{k_i})]} (\theta_{ha} - \theta_i) \quad . \tag{2.87}$$

In equation (2.86), if the temperature of the ice is held constant, the time for the humid air to come to equilibrium with the ice can be calculated. The expression for the amount of

time it takes for the temperature difference between the air and ice to be 0.1% of the initial temperature difference is

$$t = 6.91\frac{\phi_a \gamma_a C_a^{\forall} L_c}{\xi}\left(\frac{\phi_a}{k_a}+\frac{\phi_i}{k_i}\right) \quad . \tag{2.88}$$

For an air volume fraction of 0.78 which corresponds to snow density of 200 kg/m^3, an air density of 1.3 kg/m^3, a characteristic length of 1 mm, and specific surface area of 1400 m^2/m^3, the time calculated in equation (2.88) is 0.12 seconds. A similar expression can be written for the time it takes the ice to come into equilibrium with a constant air temperature. This expression is

$$t = 6.91\frac{\phi_i \gamma_i C_i^{\forall} L_c}{\xi}\left(\frac{\phi_a}{k_a}+\frac{\phi_i}{k_i}\right) \tag{2.89}$$

For the ice volume fraction of 0.22, ice density of 917 kg/m^3, and characteristic length of 1 mm, and specific surface area of 1400 m^2/m^3, the time for the temperature difference between the ice and air constituents to be 0.1% of the initial temperature difference is 65 seconds. In either case, the time for the constituents to reach equilibrium is much less than the time on the order of days that it takes for snow metamorphism to occur. In addition, condensation and evaporation of water vapor has not been taken into account in the thermal equilibration of the constituents. For example, if the air was colder than the ice and saturated with water vapor, the air would warm and the ice would cool as the two phases came into thermal equilibrium. It follows then that sublimation would occur because the air always tends to be saturated. Most of the latent heat required to make this

phase change would come from the ice phase. This would cool the ice constituent faster than without sublimation. Therefore, it is assumed that the temperatures of the ice and humid air constituents are equal.

FORMULATION SUMMARY

The conclusions of the above formulation allow the two energy equations for the pore microstructure to be added together. The energy equation for the snow with a pore microstructure can be written as

$$(\phi_a \gamma_a C_a^{\forall} + \phi_i \gamma_i C_i^{\forall}) \frac{\partial \theta_s}{\partial t} = \vec{\nabla}_x \cdot [(\phi_a k_a + \phi_i k_i) \vec{\nabla}_x \theta_s] + \hat{c} u_{sg} \tag{2.90}$$

or in one-dimension as

$$(\phi_a \gamma_a C_a^{\forall} + \phi_i \gamma_i C_i^{\forall}) \frac{\partial \theta_s}{\partial t} = \frac{\partial}{\partial x} [(\phi_a k_a + \phi_i k_i) \frac{\partial \theta_s}{\partial x}] + \hat{c} u_{sg} \tag{2.91}$$

where θ_s is the temperature of the snow. The mass supply is calculated from equation (2.48) by noting that the water vapor is always saturated at the snow temperature. The equation used to calculate the mass supply is

$$\hat{c} = \vec{\nabla}_x \cdot (\phi_v D_{v-a} \vec{\nabla}_x \gamma_v^{sat}) - \phi_v \frac{\partial \gamma_v^{sat}}{\partial t} \tag{2.92}$$

where the saturated vapor density is an exponential function of temperature. In one dimension, this equation can be written as

$$\hat{c} = \frac{\partial}{\partial x} \left(\phi_v D_{v-a} \frac{d\gamma_v^{sat}}{d\theta} \frac{\partial \theta_s}{\partial x} \right) - \phi_v \frac{d\gamma_v^{sat}}{d\theta} \frac{\partial \theta_s}{\partial t} \quad . \tag{2.93}$$

The derivative of the saturated vapor density with respect to temperature can be calculated from the equation

$$\frac{d\gamma_v^{sat}}{d\theta} = \gamma_v^{sat} \ln 10\left(\frac{2445.5646}{\theta^2} + \frac{7.2312}{\theta \ln 10} - 1.677006x10^{-2} + 2.41028x10^{-5}\theta\right) \quad (2.94)$$

where the saturated vapor density is given by Dorsey (1968) as

$$\gamma_v^{sat} = \frac{101325}{760 R_w \theta} 10^{\{\frac{-2445.5646}{\theta} + 8.2312 \log_{10}\theta - (1.677006x10^{-2})\theta + (1.20514x10^{-5})\theta^2 - 6.757169\}} \quad . \quad (2.95)$$

The above equation for the saturated vapor density was used because it provides an accurate representation of the vapor density through a broad range of temperatures.

Equation (2.93) states that condensation occurs when water vapor diffuses into areas of smaller vapor volume fraction, smaller diffusion coefficient, or into a colder area where the air cannot hold as much water. Also, any local decrease in temperature causes condensation to occur.

When equation (2.93) is substituted into equation (2.91), the equation

$$(\phi_a \gamma_a C_a^{\forall} + \phi_i \gamma_i C_i^{\forall} + u_{sg} \phi_a \frac{d\gamma_v^{sat}}{d\theta}) \frac{\partial \theta_s}{\partial t} = \frac{\partial}{\partial x}[K_{con+d}^{pore} \frac{\partial \theta_s}{\partial x}] \quad (2.96)$$

results where

$$k_{con+d}^{pore} = \phi_a k_a + \phi_i k_i + u_{sg} \phi_a D_{v-a} \frac{d\gamma_v^{sat}}{d\theta} \quad . \quad (2.97)$$

The thermal conductivity above is the effective thermal conductivity that would be measured experimentally in a mixture of ice and humid air with a pore microstructure.

The energy equation for the lamellae microstructure can be written as

$$(\phi_a \gamma_a C_a^{\forall} + \phi_i \gamma_i C_i^{\forall}) \frac{\partial \theta_s}{\partial t} = \frac{\partial}{\partial x}[k_{con}^{lam} \frac{\partial \theta_s}{\partial x}] + \hat{c} u_{sg} \quad (2.98)$$

where

$$k_{con}^{lam} = \frac{k_i k_a}{\phi_i \left(k_a + u_{sg} D_{v-a} \frac{d\gamma_v^{sat}}{d\theta} \right) + \phi_a k_i} \quad . \quad (2.99)$$

and

$$\hat{c} = \frac{\partial}{\partial x}(D_{v-a} \frac{d\gamma_v^{sat}}{d\theta} \frac{k_i}{\phi_i \left(k_a + u_{sg} D_{v-a} \frac{d\gamma_v^{sat}}{d\theta} \right) + \phi_a k_i} \frac{\partial \theta_s}{\partial x}) - \phi_v \frac{d\gamma_v^{sat}}{d\theta} \frac{\partial \theta_s}{\partial t} \quad . \quad (2.100)$$

CHAPTER III

EFFECTIVE THERMAL CONDUCTIVITIES

This chapter is concerned with comparing the two effective thermal conductivities derived in the previous chapter to experimental measurements of the thermal conductivity of snow. An effective thermal conductivity based on a linear combination of the two theoretical thermal conductivities is then hypothesized and shown to be in agreement with experimental measurements. A stereological argument is used to justify the new effective thermal conductivity model.

THEORETICAL VERSUS EXPERIMENTAL THERMAL CONDUCTIVITY

The effective thermal conductivities for the pore and lamellae microstructure are

$$k_{con+d}^{pore} = \phi_a k_a + \phi_i k_i + u_{sg}\phi_a D_{v-a}\frac{d\gamma_v^{sat}}{d\theta} \tag{3.1}$$

and

$$k_{con+d}^{lam} = \frac{k_i\left(k_a + u_{sg}D_{v-a}\dfrac{d\gamma_v^{sat}}{d\theta}\right)}{\phi_i\left(k_a + u_{sg}D_{v-a}\dfrac{d\gamma_v^{sat}}{d\theta}\right) + \phi_a k_i}\quad , \tag{3.2}$$

respectively. In Figure 3.1, several experimental correlations for effective thermal conductivity are plotted with equations (3.1) and (3.2). The experimental curves are only plotted for densities within their applicable range whereas equations (3.1) and (3.2) are plotted for densities between 0 and 917 kg/m^3 to demonstrate that they approach the

appropriate limits for thermal conductivity in pure air and pure ice. Figure 3.1 shows that equations (3.1) and (3.2) envelope the experimental correlations.

THE HYPOTHESIZED EFFECTIVE THERMAL CONDUCTIVITY MODEL

Also plotted in Figure 3.1 is the equation

$$k_s = \phi_i k_{con+d}^{pore} + \phi_a k_{con+d}^{lam} \tag{3.3}$$

where k_s is hypothesized to be the effective thermal conductivity of the snow based on a linear combination of the two extreme microstructures. Figure 3.1 shows that equation (3.3) matches the experimental correlations very well through the range of their applicable densities.

In equation (3.3), the volume fractions are now used as stereological parameters for the actual snow microstructure. Equation (3.3) implies that when the snow contains more ice, it behaves like the pore microstructure model for thermal conductivity, and when the snow contains more air, it behaves more like the lamellae microstructure model for thermal conductivity. The justification for equation (3.3) can be made by studying the snow surface section shown in Figure 3.2. When a test line is drawn through the surface section, a fraction of the total length will pass through the ice constituent, and the remainder will pass through the humid air constituent. The fraction that intersects the ice constituent is approximately the volume fraction of the ice, and the remaining fraction is the volume fraction of the humid air constituent. Anytime the test line passes through the ice, heat transfer along that portion of the line occurs like in the pore microstructure, that

is, in parallel with the air phase. Also anytime the test line passes through the humid air constituent, heat transfer is occurring like that in the lamellae microstructure or in series with the ice phase. Therefore, it was hypothesized that the thermal conductivity of the snow could be modeled as the linear combination of the effective thermal conductivities

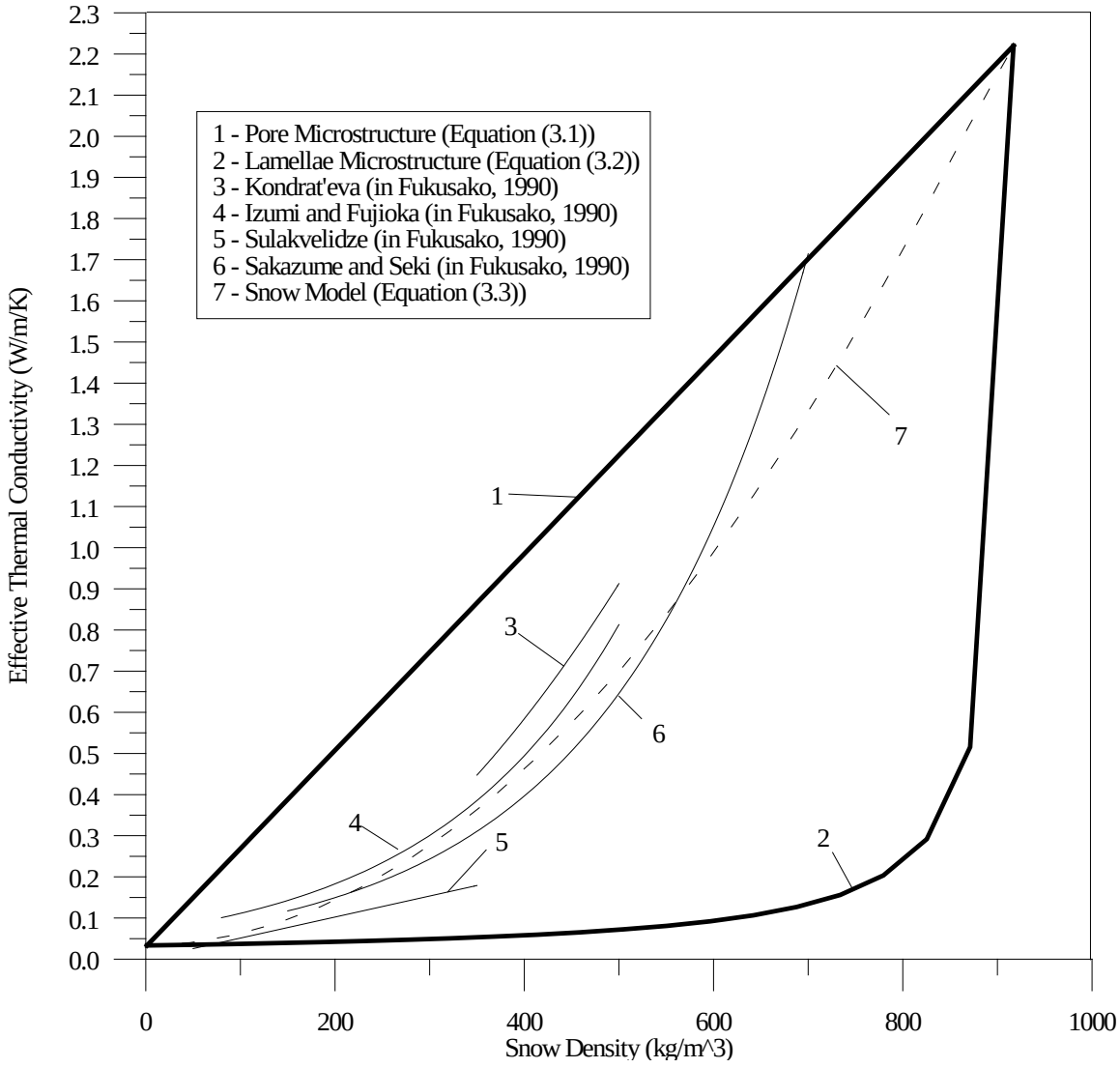

Figure 3.1. Effective Thermal Conductivites for Ideal Microstructures, Actual Snow, and the Proposed Model at -10^{o} C.

for the two microstructure extremes simply scaled by the volume fraction of each constituent.

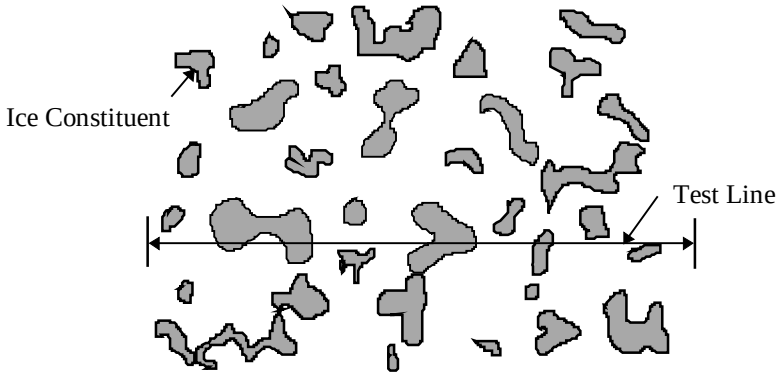

Figure 3.2. Surface Section of Snow.

MODEL EQUATIONS

The energy equation used for the snow model based on equations (2.91) and (2.98) is

$$(\phi_a \gamma_a C_a^{\forall} + \phi_i \gamma_i C_i^{\forall}) \frac{\partial \theta_s}{\partial t} = \frac{\partial}{\partial x}[k_{con}^s \frac{\partial \theta_s}{\partial x}] + \hat{c} u_{sg} \tag{3.4}$$

where

$$k_{con}^s = \phi_i (\phi_a k_a + \phi_i k_i) + \phi_a \frac{k_i k_a}{\phi_i \left(k_a + u_{sg} D_{v-a} \frac{d\gamma_v^{sat}}{d\theta} \right) + \phi_a k_i} \quad . \tag{3.5}$$

The above effective thermal conductivity is based on equation (3.3) without the diffusion effects. Based on equations (2.48) and (2.49), the mass supply is calculated from the equation

$$\hat{c} = \frac{\partial}{\partial x}(D_s \frac{d\gamma_v^{sat}}{d\theta} \frac{\partial \theta_s}{\partial x}) - \phi_v \frac{d\gamma_v^{sat}}{d\theta} \frac{\partial \theta_s}{\partial t} \tag{3.6}$$

where D_s is the diffusion coefficient in snow given by

$$D_s = \phi_i\left(\phi_a D_{v-a}\right) + \phi_a\left(\frac{D_{v-a}k_i}{\phi_i\left(k_a + u_{sg}D_{v-a}\frac{d\gamma_v^{sat}}{d\theta}\right) + \phi_a k_i}\right) \quad . \tag{3.7}$$

In equations (3.5)-(3.7), the conduction and diffusion contributions to the effective thermal conductivity of equation (3.3) have been separated by keeping the mass supply term in the energy equation. This will allow the mass supply to be calculated explicity from equation (3.6), which is useful when studying depth hoar crystal growth. The diffusion coefficient in snow is a disputed number in that some researchers have claimed it is less than the diffusion coefficient in air (Giddings & LaChapelle, 1962) due to the fact that the ice grains in the snow interfere with the diffusion. Experiments by Yosida *et al.* (1955, in Colbeck, 1993) showed that the diffusion coefficient was 3.5 to 5 times as large while the experiments of Sommerfeld et al. (1986, in Colbeck, 1993) found that the diffusion coefficient in snow was about twice that for air. The diffusion coefficient given by equation (3.7) divided by the diffusion coefficient in air is plotted in Figure 3.3 to show its enhancement as a function of snow density at a snow temperature of -10^o C. The diffusion enhancement for this model was found to be a maximum of about 1.23 times the diffusion of water vapor in air. This enhancement may be small compared to the latest experimental results, however, given the lack of concensus of what the diffusion coefficient in snow actually is, this model will serve the purpose of the goals to be achieved in this thesis. Moreover, equation (3.7) demonstrates some plausible

characteristics in that it approaches the correct limits for the cases of pure air and pure ice. It also increases for snow densities up to 500 kg/m^3 and then decreases for densities up to the pure ice density of 917 kg/m^3. This is plausible because the ice grains in the snow are bound to inhibit diffusion due to a tortuosity effect at high snow densities.

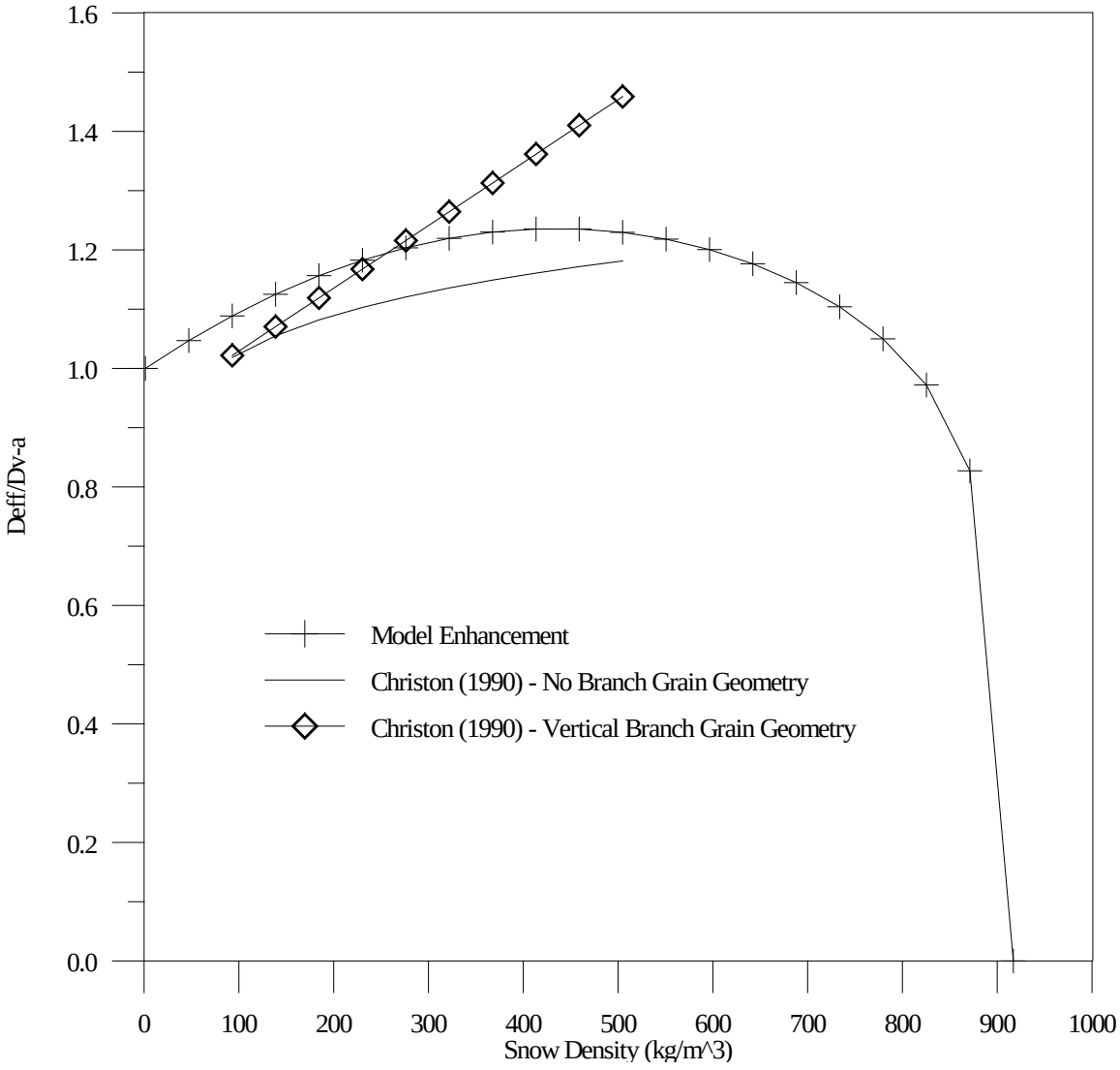

Figure 3.3. Effective Diffusion Coefficient Enhancement as a Function of Density at a Temperature of -10^o C.

Also plotted in Figure 3.3 are Christon's (1990) diffusion enhancement ratios for two geometries in their applicable density ranges. In Christon's 1990 work, he developed a three-dimensional heat and mass transfer model for a single lattice cell in snow. He then calculated effective thermal conductivites and diffusion coefficients. In Figure 3.3, two of his correlations for the no-branch geometry and his vertical branch geometry are plotted. The model given by equation (3.7) lies within a reasonable distance of Christon's correlations given the uncertainty of this parameter.

CHAPTER IV

NUMERICAL FORMULATION

This chapter presents the development of the numerical formulation to solve the equations of heat and mass transfer in snow. The FORTRAN program used to solve these equations is also described. The formulation presented solves a general one-dimensional parabolic partial differential equation. The Galerkin finite element method is used to discretize the spatial domain, and the Crank-Nicolson time integration method is used in the time domain.

GENERAL PARABOLIC EQUATION

The general parabolic equation that this formulation uses is

$$m(x,t)\frac{\partial\theta}{\partial t} = \frac{\partial}{\partial x}\left(p(x,t)\frac{\partial\theta}{\partial x}\right) - \omega(x,t)\theta + f(x,t) \quad . \tag{4.1}$$

The energy equation for snow is of this form. Either the dependent variable can be specified at a boundary or the heat flux can be specified as

$$-p(a,t)\left.\frac{\partial\theta}{\partial x}\right|_{x=a} = A(t) \tag{4.2a}$$

at the left boundary and

$$p(b,t)\left.\frac{\partial\theta}{\partial x}\right|_{x=b} = B(t) \tag{4.2b}$$

at the right boundary.

The initial condition is

$$\theta(x,0) = \theta_o(x) \quad . \tag{4.3}$$

FINITE ELEMENT FORMULATION

The first step in the numerical formulation is the discretization of the domain. The domain consists of equally spaced nodes as shown in Figure 4.1. The dependent variable will be approximated by quadratic interpolation and may be expressed as

$$\theta(x,t) = \sum_{j=1}^{N+1} \theta_j(t) n_j(x) \tag{4.4}$$

where θ_j are the nodal values of the dependent variable which are a function of time and $n_i(x)$ are the quadratic interpolation functions. The elemental formulation is based on the weak statement which is

$$\int_a^b \left[\left(p\theta' \right)' - q\theta + f - m\dot{\theta} \right] \nu dx = 0 \tag{4.5}$$

where ν is a test function satisfying the essential boundary conditions, the prime denotes

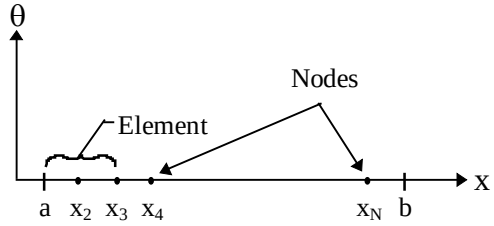

Figure 4.1. Nodes for the Spatial Domain.

differentiation with respect to the spatial variable, and the dot denotes differentiation with respect to time. Integrating equation (4.5) by parts and eliminating the derivative terms from the boundary conditions yields

$$\int_a^b \left(p\theta'\nu' + q\theta\nu + m\dot{\theta}\nu\right)dx = \int_a^b f\nu dx + A(t)\nu(a) + B(t)\nu(b) \quad . \tag{4.6}$$

Substitution of the quadratic approximation of the dependent variable and setting

$$\nu = n_k, \quad k = 1,2,\ldots,N+1 \tag{4.7}$$

gives

$$\begin{aligned}\sum_{j=1}^{N+1}\left[\left(\int_a^b n_k' p n_j' + n_k q n_j dx\right)u_j(t) + \left(\int_a^b n_k m n_j dx\right)\dot{u}_j(t)\right] \\ = \int_a^b f n_k dx + A(t)\delta_{k1} + B(t)\delta_{kN+1}, \quad k = 1,2,\ldots,N+1\end{aligned} \tag{4.8}$$

which can be written in matrix form as

$$\mathbf{A}\theta + \mathbf{B}\dot{\theta} = \mathbf{f} \tag{4.9}$$

where

$$\mathbf{A} = \sum_e \left(\mathbf{p}_e + \mathbf{q}_e\right) \quad , \tag{4.10}$$

$$\mathbf{B} = \sum_e \mathbf{m}_e \quad , \tag{4.11}$$

$$\mathbf{f} = \sum_e \mathbf{f}_e + \mathbf{bc} \quad , \tag{4.12}$$

with

$$\mathbf{p}_e = \int_{x_i}^{x_{i+2}} \mathbf{n}' p \mathbf{n}'^{\mathrm{T}} dx \quad , \tag{4.13}$$

$$\mathbf{q}_e = \int_{x_i}^{x_{i+2}} \mathbf{n} q \mathbf{n}^{\mathrm{T}} dx \quad , \tag{4.14}$$

$$\mathbf{m}_e = \int_{x_i}^{x_{i+2}} \mathbf{n} m \mathbf{n}^{\mathrm{T}} dx \quad , \tag{4.15}$$

$$\mathbf{f}_e = \int_{x_i}^{x_{i+2}} f\mathbf{n}dx \quad , \tag{4.16}$$

and

$$\mathbf{bc}^T = \left[A(t) \quad 0 \quad 0 \quad \ldots \quad 0 \quad 0 \quad B(t)\right] \quad . \tag{4.17}$$

When the functions p, q, m, and f can be approximated by quadratic functions on an element, the components of the element matrices $\mathbf{p}_e$, $\mathbf{q}_e$, and $\mathbf{m}_e$ and vector $\mathbf{f}_e$ are easily calculated based on the nodal values of the functions p, q, m, and f. The evaluated integrals are given in Bickford (1990).

When natural boundary conditions are specified, no further modification of the coefficient matrices is needed. When essential boundary conditions are specified, the coefficient matrix and load vector are modified after the time integration scheme is employed.

The Crank-Nicolson time integration scheme (Bickford, 1990) was used to integrate equation (4.9). The method gives an accumulated discretization error on the order of the time differential h^2 and is also unconditionally stable. This method is employed by approximating the time derivative by evaluating it at the endpoints of the time interval and taking the average. For the vector equation (4.9), the corresponding expression is

$$\theta_{n+1} = \theta_n + \frac{h\left(\dot{\theta}_n + \dot{\theta}_{n+1}\right)}{2} \quad . \tag{4.18}$$

After multiplying equation (4.18) through by **B** and using equation (4.9), the Crank-Nicolson algorithm can be written as

$$\left(\mathbf{B}+\frac{h\mathbf{A}}{2}\right)\theta_{n+1}=\left(\mathbf{B}-\frac{h\mathbf{A}}{2}\right)\theta_{n}+\frac{h\left(\mathbf{f}_{n}+\mathbf{f}_{n+1}\right)}{2} \quad . \tag{4.19}$$

or

$$\mathbf{K}\theta_{n+1}=\mathbf{b}_{n+1} \tag{4.20}$$

where

$$\mathbf{K}=\mathbf{B}+\frac{h\mathbf{A}}{2} \tag{4.21}$$

and

$$\mathbf{b}_{n+1}=\left(\mathbf{B}-\frac{h\mathbf{A}}{2}\right)\theta_{n}+\frac{h\left(\mathbf{f}_{n}+\mathbf{f}_{n+1}\right)}{2} \quad . \tag{4.22}$$

The essential boundary conditions can now be applied to the system (4.20) by the penalty method where the left-upper corner and right-lower corner elements are multiplied by a large number, say 10^{15}. The first and last elements in the load vector $\mathbf{b}_{n+1}$ are set to the specified essential boundary condition and then multiplied by the coefficient matrix element-large number product. The first and last equations of the system then consist of

$$10^{15}K_{11}\theta_{1}+K_{12}\theta_{2}+\ldots+K_{1,N+1}\theta_{N+1}=10^{15}K_{11}\theta(a,t) \tag{4.23}$$

and

$$K_{N+1,1}\theta_{1}+K_{12}\theta_{2}+\ldots+10^{15}K_{N+1,N+1}\theta_{N+1}=10^{15}K_{N+1,N+1}\theta(b,t) \quad . \tag{4.24}$$

The first term on the left hand side in equation (4.23) and the last term in equation (4.24) are large compared to the other terms in these equations except the right-hand side terms, so these equations are effectively

$$\theta_1 = \theta(a,t)$$

and

$$\theta_{N+1} = \theta(b,t)$$

which are the desired essential boundary conditions. When the heat flux is specified, no modifications are necessary because this is taken care of automatically in the assembly process.

The mass supply is calculated for the one-dimensional case by the equation

$$\hat{c} = \frac{\partial}{\partial x}\left(D_s \frac{d\gamma_v^{sat}}{d\theta}\frac{\partial \theta_s}{\partial x}\right) - \phi_v \frac{d\gamma_v^{sat}}{d\theta}\frac{\partial \theta_s}{\partial t} \quad . \tag{4.25}$$

The spatial derivatives in this equation are approximated by second-order accurate finite difference formulas. Forward and backward difference formulas are used at the boundaries, and the central difference formula is used in the interior of the spatial domain. The time derivative is approximated by a first-order accurate, backward difference formula.

DESCRIPTION OF FORTRAN CODE

A FORTRAN program was written to solve the coupled set of equations (4.1) and (4.25). The program is contained in Appendix A and performs the following steps to obtain the temperature distribution as a function of space and time:

1. Reads boundary conditions and initial conditions from data file.

2. Initializes all arrays.

3. Calculates the mass supply based on previous iteration's temperature distribution. The first guess for the new time step is the previous time step's solution.

4. Calculates the coefficients m, p, and q to the original differential equation (4.1) at regularly spaced time intervals.

5. Calculates the forcing function f based on the previous time step solution and previous iteration solution as needed for the Crank-Nicolson time integration scheme.

6. Calculates a new solution at the current time with the Crank-Nicolson time integration scheme.

7. Checks for convergence by the L2 norm at the current time step by comparing the new solution to the previous iteration's solution.

8. If not converged, then repeats steps 3-7.

9. If converged, then calculates a new ice volume fraction based on the converged value of the mass supply.

10. Records the solution in a data file at specified times.

11. Stores the current time solution in arrays to be used at the next time step.

12. Repeats steps 2-11 until a specified time limit is reached.

CHAPTER V

NUMERICAL RESULTS

This chapter describes the code verification and the numerical results given by the program described in Chapter IV. The problem at hand is to model the heat and mass transfer in a snowpack 1 meter deep with the complexities associated with a real snowpack such as dense layers and a varying surface boundary condition. Figure 5.1 shows the domain in which the energy equation for snow is solved.

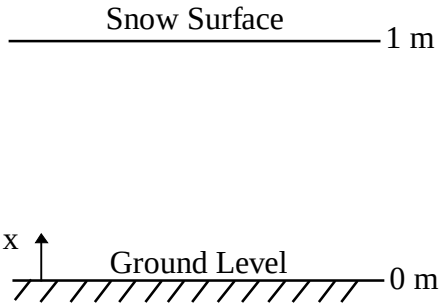

Figure 5.1. The Domain Orientation for the Solution of Heat and Mass Transfer in Snow.

CODE VERIFICATION

Before proceeding to solve the nonlinear heat equation coupled with the mass supply, several test problems with known analytical solutions were solved by the program. The first problem solved by numerical solution was the time dependent diffusion equation with Dirichlet boundary conditions and a homogeneous initial condition given by

$$\frac{\partial \theta}{\partial t} = \frac{k}{\gamma C} \frac{\partial^2 \theta}{\partial x^2} \quad , \tag{5.1}$$

$$\theta(0,t) = 0^{o}\,C \quad t \geq 0, \tag{5.2}$$

$$\theta(1,t) = 1^{o}\,C \quad t \geq 0, \tag{5.3}$$

and

$$\theta(x,0) = 0^{o}\,C \quad 0 \leq x \leq 1. \tag{5.4}$$

Figure 5.2 shows that the numerical solution agrees very well with the analytical solution.

The next problem solved by the numerical solution was the time dependent diffusion equation with an internal generation term dependent on space and time. The boundary conditions were of the Dirichlet type and the initial condition was homogeneous.

The equation and associated boundary conditions were

$$\frac{\partial\theta}{\partial t} = \frac{k}{\gamma C}\frac{\partial^{2}\theta}{\partial x^{2}} + \Gamma x t \tag{5.5}$$

where Γ is a constant,

$$\theta(0,t) = 0^{o}C \quad t \geq 0, \tag{5.6}$$

$$\theta(1,t) = -20^{o}C \quad t \geq 0, \tag{5.7}$$

and

$$\theta(x,0) = 0^{o}C \quad 0 \leq x \leq 1 \quad . \tag{5.8}$$

Figure 5.3 shows that the numerical solution agrees very well with the analytical solution.

Finally, in order to check the time varying boundary condition complexity to the problem, equation (5.1) was solved with the time dependent surface boundary condition given by

$$\theta(1,t) = -10 - 10\sin\left(\frac{\pi}{43200}t\right) \quad . \tag{5.9}$$

This solution was plotted in Figure 5.4. The exact solution (Colbeck, 1989) given by

$$\theta(x,t) = -10 - 10e^{-(1-x)\left(\omega/2\lambda\right)^{1/2}} \sin\left(\omega t - (1-x)\left(\omega/2\lambda\right)^{1/2}\right) \tag{5.10}$$

where

$$\lambda = \frac{k}{\gamma C} \tag{5.11}$$

and

$$\omega = \frac{2\pi}{86400} \tag{5.12}$$

laid right over the top of the numerical solution, so it was not plotted in Figure 5.4. These test cases lend confidence to the accuracy of the numerical code.

SNOWPACK RESULTS

The numerical results corresponding to two test cases for a snowpack are presented in this section. Colbeck (1991) stressed the importance of developing a theory of snow which incorporates the effect of layers on the heat transfer in snow. The model snowpacks presented contain dense layers. The volume fraction of the ice is the

dependent variable which allows the density to be a function of position in the snowpack. The density of the snow is calculated from the equation

$$\rho_s = \phi_i \gamma_i + (1 - \phi_i)\gamma_{ha} \quad . \tag{5.13}$$

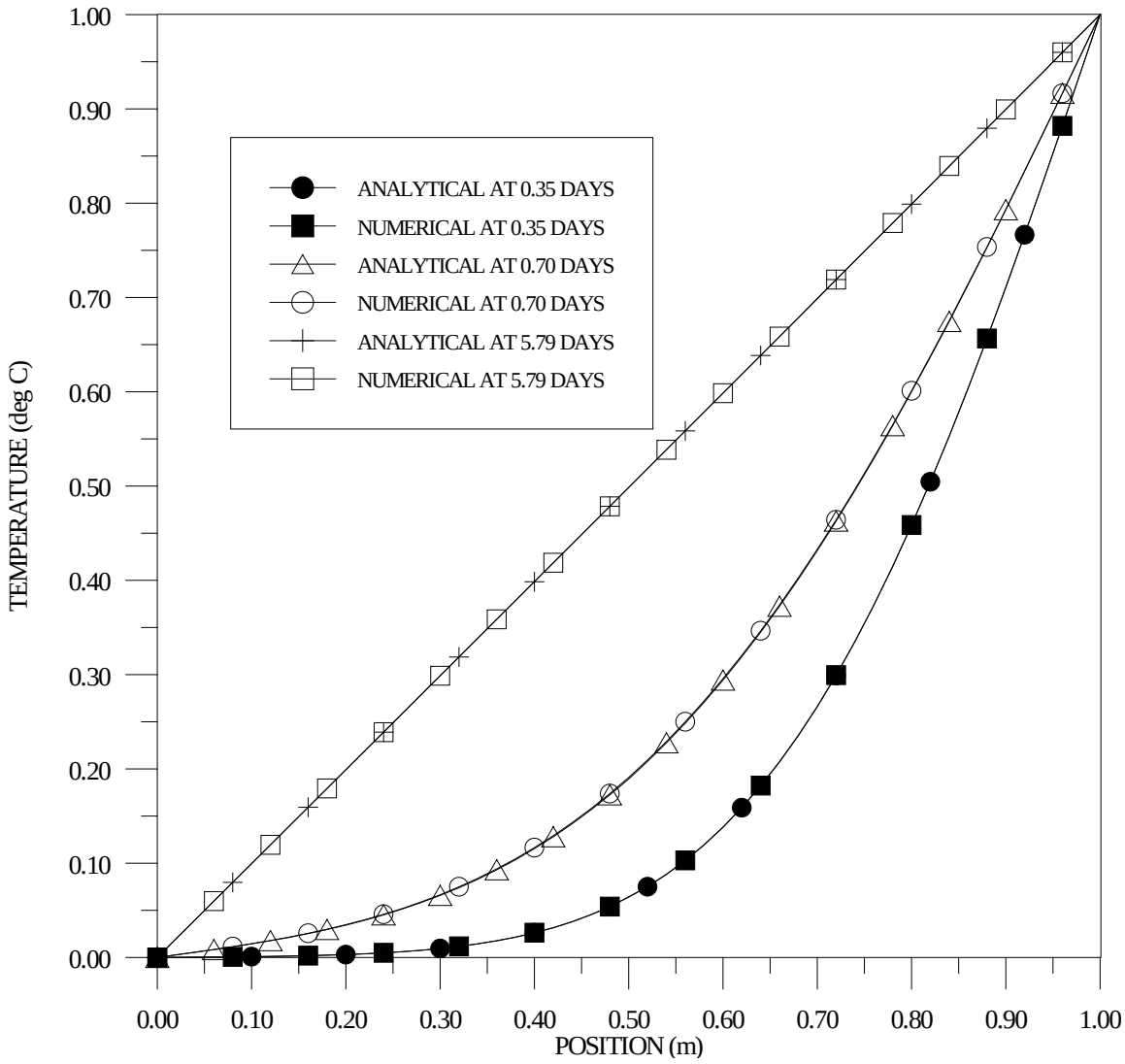

Figure 5.2. Comparison of Analytical Solution to Numerical Solution for a Simple Diffusion Problem.

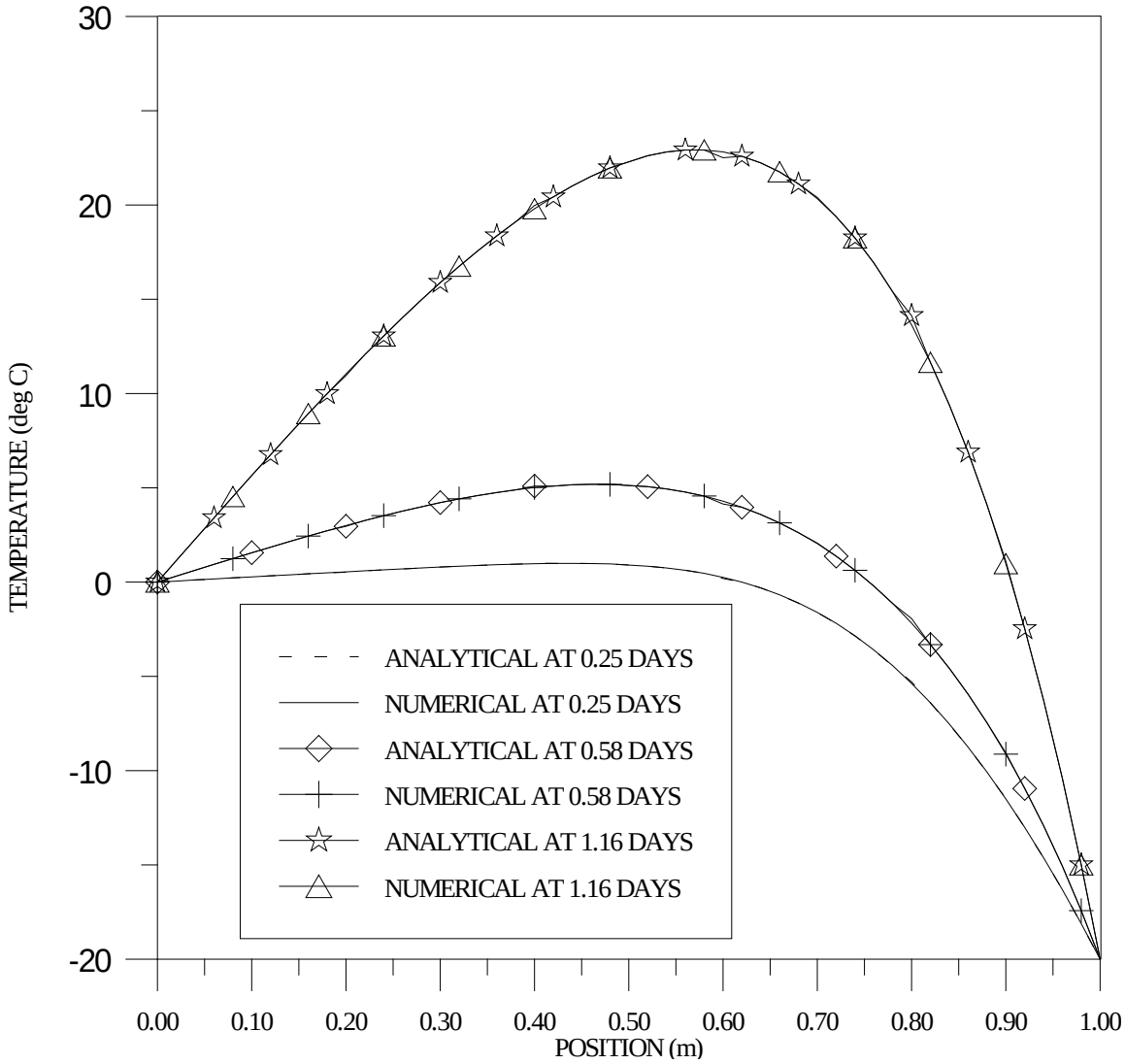

Figure 5.3. Comparison of Analytical Solution to Numerical Solution for a Diffusion Problem with Space and Time Dependent Heat Generation.

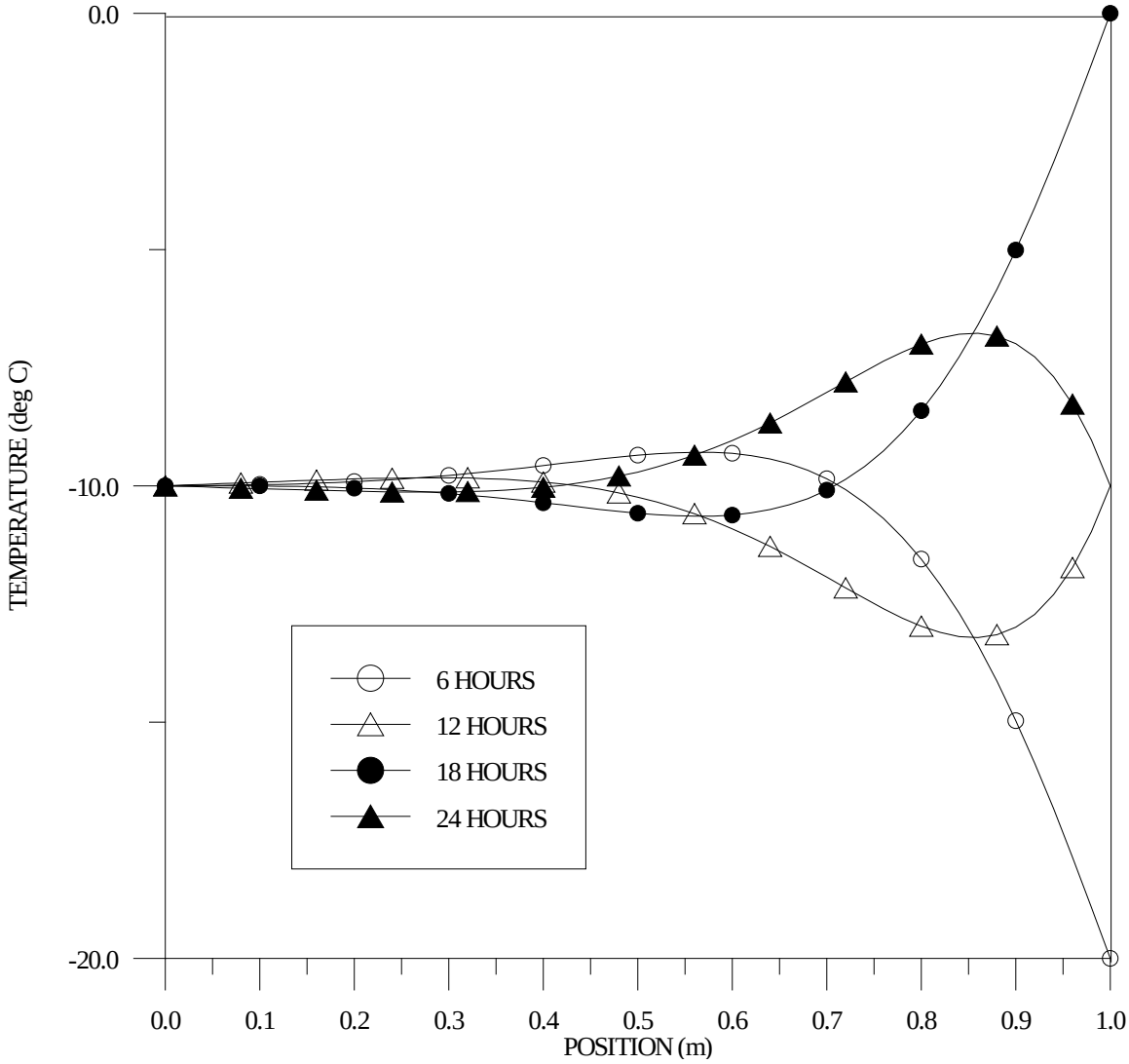

Figure 5.4. Code Verification for Time Dependent Boundary Condition.

CONSTANT BOUNDARY CONDITIONS. The first test case involved a 1 m deep snowpack with a dense layer starting at 64 cm and ending at 86 cm. Figure 5.5 shows the ice volume fraction profile. The snow had a density of 200 kg/m^3 with an increase over 8 cm to a density of 605 kg/m^3. The ice volume fraction at the ground level was set to one. The solid ice at the ground layer is believed to be a more realistic model of actual snowpack conditions. If the volume fraction of the ice is set to a number less than one, then the snowpack can be viewed as having no barriers below it. In other words, the model predicts that saturated air enters the snowpack at the ground level with no specified source for this vapor. The initial conditions on the snowpack were isothermal at 0^o C, and the boundary conditions at the bottom and top surfaces were 0^o C and -20^o C, respectively.

Figure 5.6 is the temperature profile in the snowpack for various times up to steady-state at 20 days. In the dense layer of the snow, the temperature gradient is noticeably reduced at any time during the transient state. This is due to the higher thermal conductivity of the dense snow. The temperature profile near the surface is steep at one day, and as can be seen in Figure 5.7, the condensation rate of the water vapor at day one is also high near the surface. This is because water vapor is diffusing toward the surface which is colder and, therefore, an area of lower saturation. The water vapor must then condense if the air is not to become supersaturated. Also the local temperature near the surface is decreasing rapidly which means that the water vapor must condense to keep the air at saturation. Just below the dense layer, Figure 5.7 shows a peak in condensation

rate during the transient stage and at steady-state. This is due to the decrease in cross-sectional area in the direction of the water vapor diffusion. If the amount of air available to hold water decreases, then the amount of water vapor must also decrease. Just above

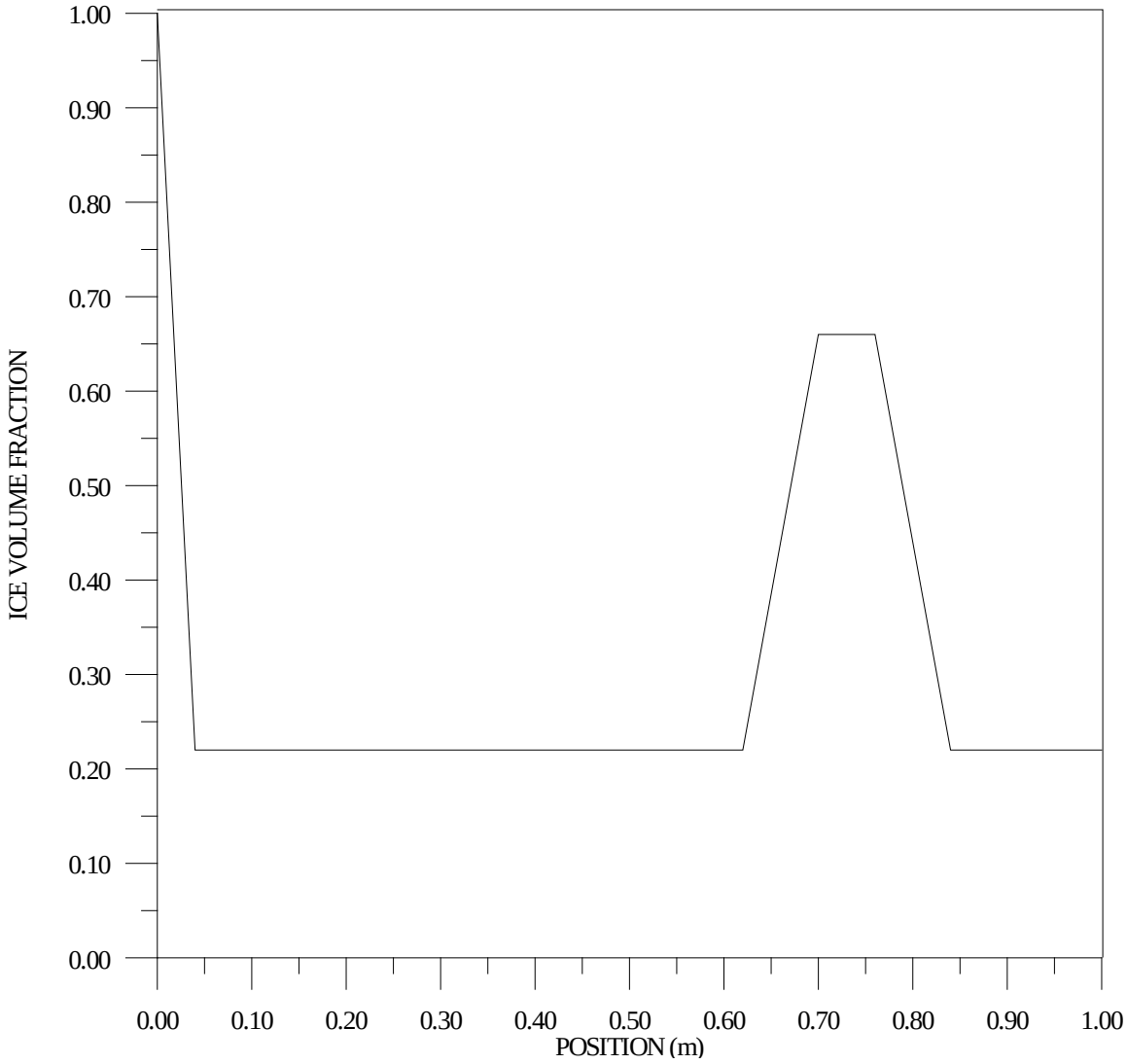

Figure 5.5. Ice Volume Fraction Profile in Snowpack.

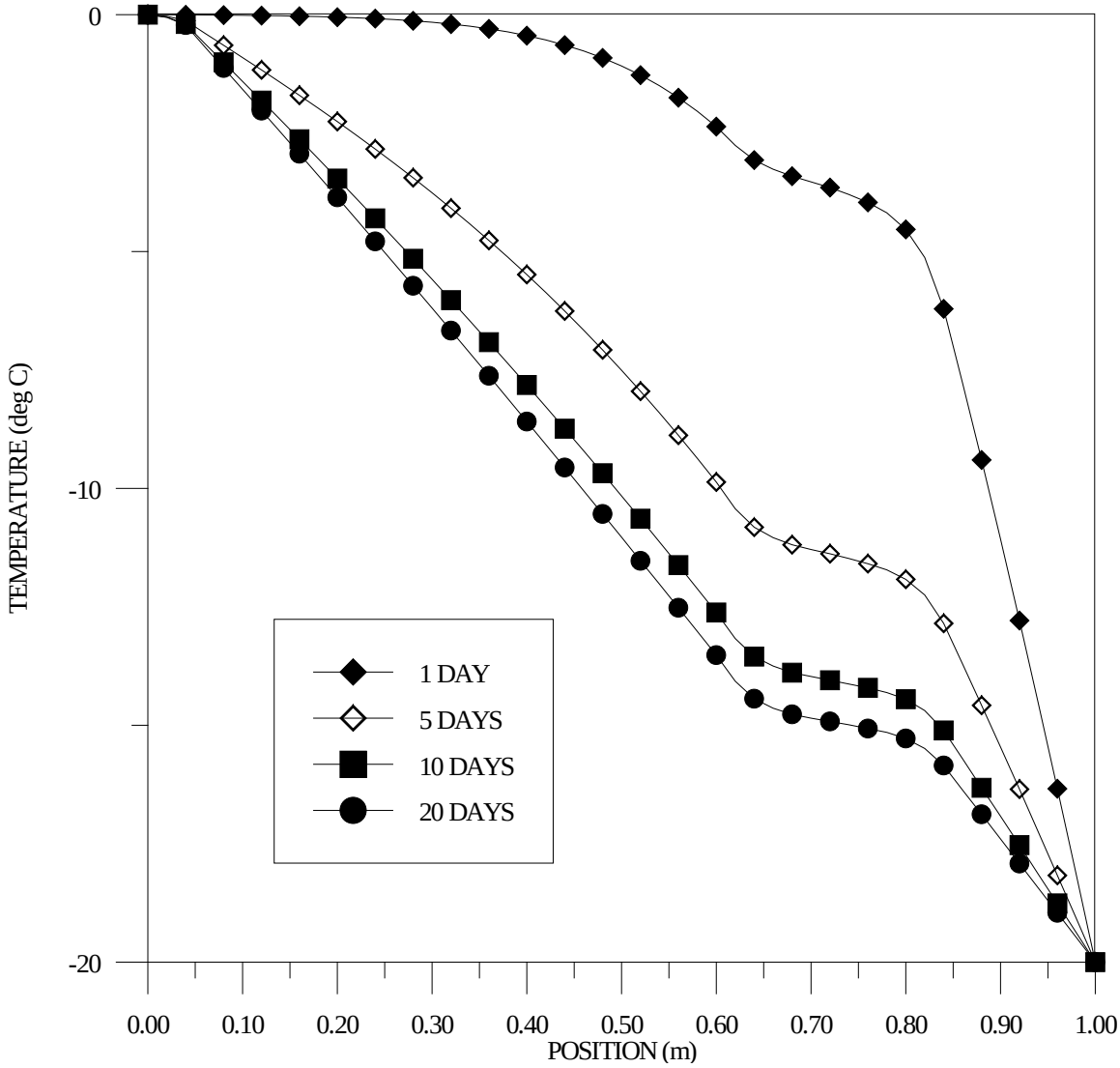

Figure 5.6. Temperature Profile in a Snowpack with a Dense Layer.

the dense layer, the opposite is true. Figure 5.7 shows that evaporation is occurring because the vapor volume fraction is increasing in the direction of vapor flow. Evaporation must occur to keep the increasing amount of air saturated.

Local weakening above and below dense layers has been observed (Adams and

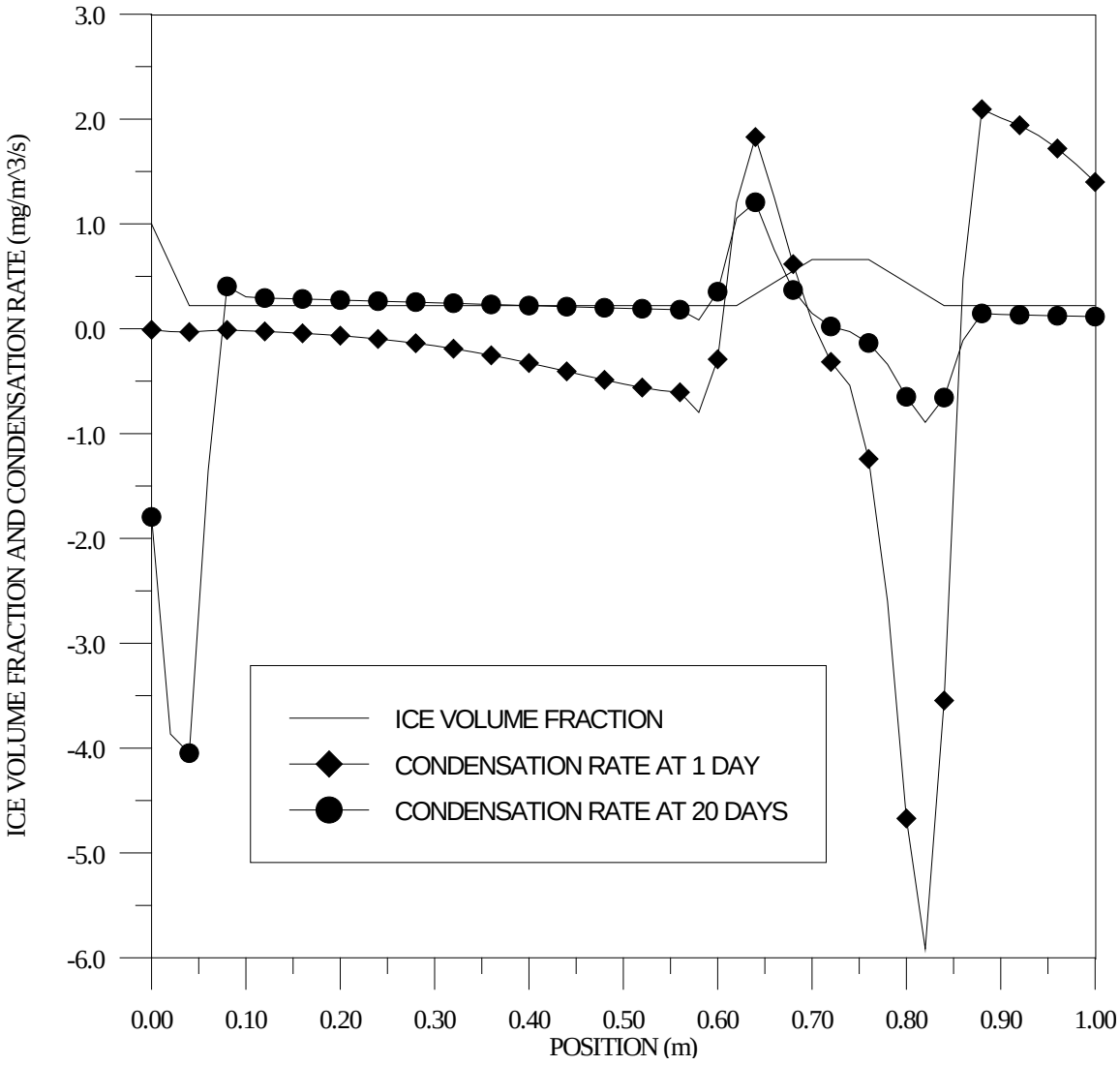

Figure 5.7. Condensation Rate in a Snowpack with a Dense Layer.

Brown, 1982). If condensation is known to enhance depth hoar growth (Colbeck, 1983), then the condensation occurring below the dense layer in Figure 5.7 could contribute to the weakening observed in this region of an experimental snowpack. The evaporation occurring above the dense layer may contribute to the weakening observed here. At the

steady-state evaporation rate just above the dense layer in Figure 5.7, a decrease in density of 1 kg/m^3 would take about 14 days. This is a fairly slow rate of evaporation but could be enhanced in a real environment by larger temperature gradients, transient conditions, or steeper density gradients. In fact, at the maximum rate of evaporation during the transient stage in Figure 5.7, a 1 kg/m^3 density drop could occur in 2-3 days.

TIME DEPENDENT BOUNDARY CONDITION. In this case, a 1 m deep snowpack was subjected to a harmonic temperature boundary condition at the snow surface given by

$$\theta_s(1,t) = -20 - 10\sin\left(\frac{\pi}{43200}t\right) \quad . \tag{5.14}$$

The above equation is used as a model of the diurnal fluctuations in air temperature. The boundary condition given by equation (5.14) has a mean value of -20^o C with a $\pm 10^o$ C fluctuation about the mean. Again the dense snow layer was included at the same position as in the previous test case.

Figure 5.8 shows the temperature profile in the snowpack after the transients have disapppeared. The temperature above the dense layer fluctuates a great deal, but the temperature in the dense layer and below fluctuates much less. The dense layer has the effect of reducing the temperature gradient in the dense snow. Figure 5.9 shows the temperature profile in a snowpack without a dense layer but with the same fluctuating boundary condition (equation 5.14) at the surface. By examining Figures 5.8 and 5.9, the penetration depths of the temperature fluctuations for the two cases are about equal

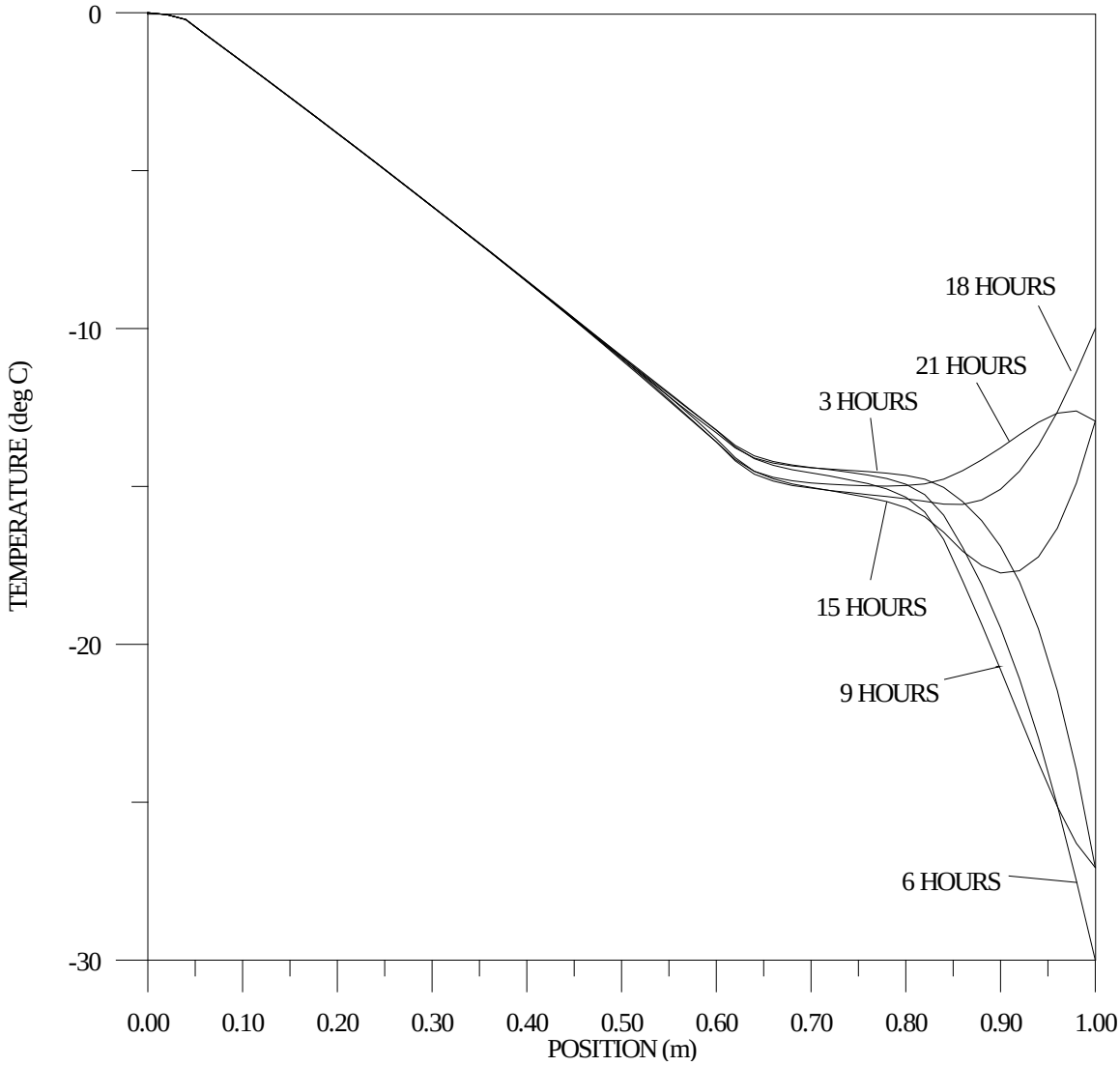

Figure 5.8. Temperature Profile in a Snowpack with a Dense Layer and Time Dependent Surface Boundary Condition.

The temperature gradients can be very large during daily variations in surface temperature as shown in Figure 5.8. Large temperature gradients not only increase depth hoar rate of growth (Colbeck, 1983) due to condensation and sublimation amongst neighboring ice particles, but also increase the rate of condensation and evaporation as shown in Figure 5.9. Colbeck (1989) noted that depth hoar growth has been observed

close to the surface in some snowpacks. The large temperature gradients imposed by daily changes in surface temperature are one likely cause as Figures 5.8 and 5.9 demonstrate.

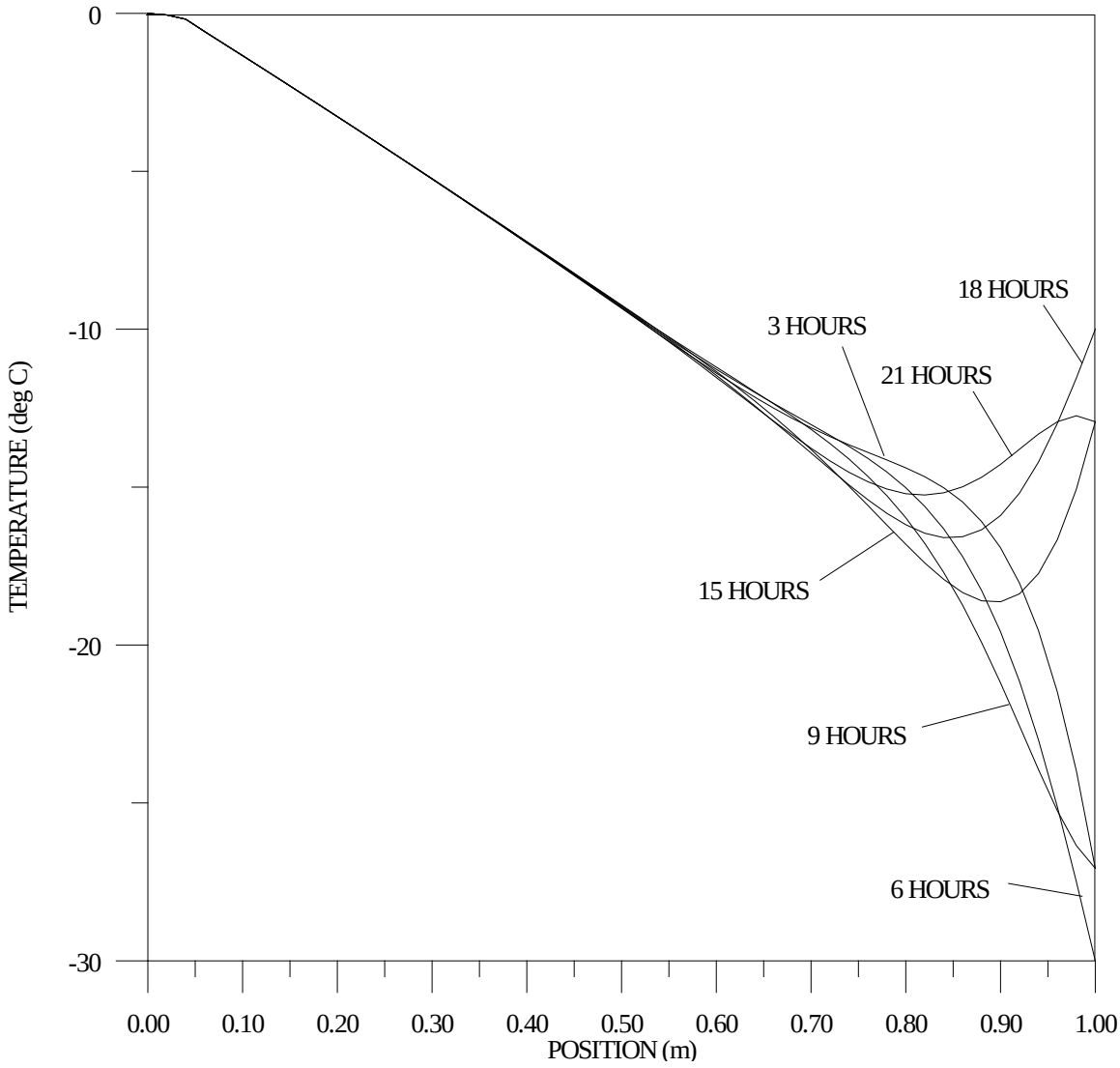

Figure 5.9. Temperature Profile in a Snowpack with Time Dependent Surface Boundary Condition but without a Dense Layer.

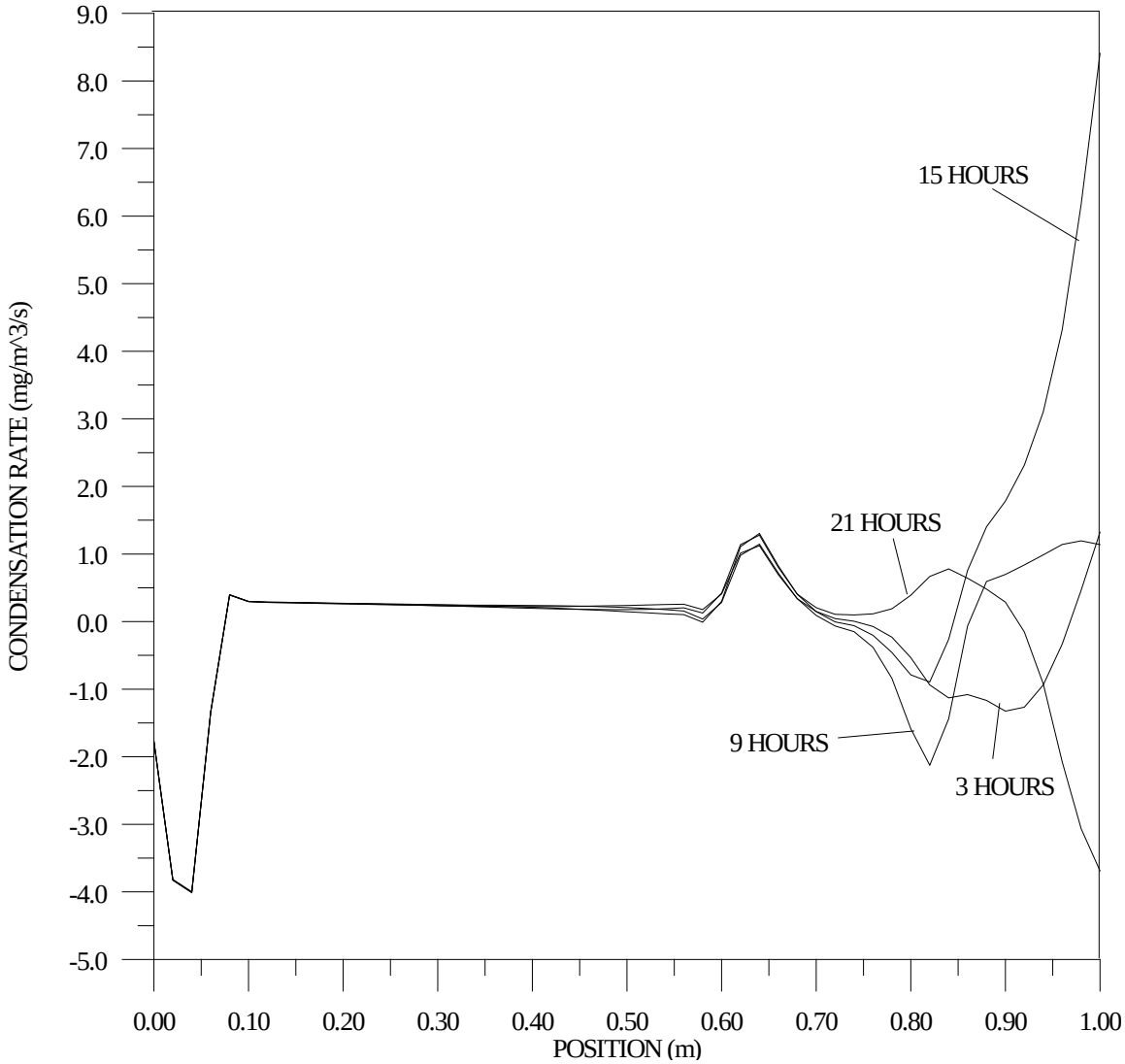

Figure 5.10. Condensation Rate in a Snowpack with a Dense Layer and Time Dependent Surface Boundary Condition.

CHAPTER VI

CONCLUSIONS AND RECOMMENDATIONS

Temperature gradient metamorphism of snow has been shown to be a factor in the release of many avalanches. This process is an active growth of a characteristic type of crystal called depth hoar which forms in the presence of a temperature gradient. The temperature gradient induces heat and mass transfer through the snowpack. Previous work in this area has produced useful results when the microstructure was considered or when a homogeneous snowpack was considered. A modern mixture theory was chosen to model the heat and mass transfer process with the intent to lay the groundwork for a unified model of snow in that macroscopic effects would together be considered with microstructural evolution. Furthermore, previous success with the modern mixture theory had been attained in modeling composite materials. In order to broaden its range of application, it was applied here to a heat and mass transfer problem.

The modern mixture theory presented has been successfully applied to the heat and mass transfer problem of temperature gradient metamorphism of snow. Two ideal microstructures for the snow were considered that envelope the range of possible microstructures in the snow. Effective thermal conductivities and diffusion coefficients were obtained from these microstructures. A linear combination of the results from these two microstructures was then used as the effective thermal conductivity in the snow. Comparison with experimental effective thermal conductivities showed this is a

reasonable model for the effective thermal conductivity of the snow. The effective diffusion coefficient for the water vapor was also shown to be enhanced over the normal diffusion coefficient for water vapor in air up to a snow density of about 800 kg/m^3.

The theory developed for the heat and mass transfer in snow is believed to be the most coherent in that it was derived from one general theory. Some terms in previous researchers equations were not clearly derived. The groundwork has been formulated here for a more complete understanding of the heat and mass transfer in snow by presenting a complete development of the governing equations.

A numerical method was developed based on the Galerkin finite element method and Crank-Nicolson time integration scheme to solve the governing equations for heat and mass transfer in snow. The numerical method obtains second order accuracy in both the spatial and time domains. Furthermore, the numerical method is general enough to handle any such complexities that are associated with a snowpack in a real environment such as time varying boundary conditions, time dependent internal heat generation due to solar radiation, and nonlinearity of the coefficients in the differential equation.

The numerical method was then tested by using it to solve parabolic differential equations in one-dimension that had known analytical solutions. The numerical solutions agreed very well with the known analytical solutions. Once confidence in the numerical method was established, it was used to solve the equations governing heat and mass transfer in snow. The model snowpack contained a dense layer as real snowpacks often do. The results showed that the dense layer causes water vapor to condense below it and

ice to sublimate above it. This may correlate with experimental observations that have shown significant snowpack weakening above and below dense layers in experimental snowpacks. It was also shown that a time varying temperature boundary condition at the snow surface induces large fluctuations in temperature gradient and condensation rate of the water vapor which both contribute to the growth of depth hoar. Depth hoar growth near the surface has been observed in real snowpacks.

Further research needs to be done in the area of stereology of snow to quantify the effective thermal conductivities and diffusion coefficients based on easily identifiable stereological variables. A microstructure evolution model must then be developed based on the macroscopic variables calculated in the theory presented here such as temperature gradient and condensation rate. When the microstructure evolves, the effective thermal conductivities and diffusion coefficients change. Incorporating all these considerations into the groundwork established in this thesis would be the next step in developing a unified model of snow.

LITERATURE CITED

Adams, E.E. & Brown, R.L. (1982). Further results on studies of temperature gradient metamorphism. Journal of Glaciology, 28 (98), 205-209.

Adams, E.E. & Brown, R.L. (1989). A constitutive theory for snow as a continuous multiphase mixture. International Journal of Multiphase Flow, 15 (4), 553-572.

Adams, E.E. & Brown, R.L. (1990). A mixture theory for evaluating heat and mass transport processes in nonhomogeneous snow. Continuum Mechanics and Thermodynamics, 2, 31-63.

Bedford, A. & Drumheller, D.S. (1983). Recent advances: theories of immiscible and structured mixtures. International Journal of Engineering Science, 21 (8), 863-960.

Bickford, W.B. (1990). A First Course in the Finite Element Method. Homewood, IL: IRWIN.

Bird, R.B., Stewart, W.E., & Lightfoot, E.N. (1960). Transport Phenomena. New York: John Wiley & Sons.

Bradley, C.C., Brown, R.L., & Williams, T.R. (1977). Gradient metamorphism, zonal weakening of the snow-pack and avalanche initiation. Journal of Glaciology, 19 (81), 335-342.

Christon, M. (1990). 3-D transient microanalysis of multi-phase heat and mass transport in ice lattices (Doctoral dissertation, Mechanical Engineering Department, Colorado State University, 1990).

Colbeck, S.C. (1982). Growth of Faceted Crystals in a Snow Cover. U.S. Army Cold Regions Research and Engineering Laboratory. (CRREL Report 82-29).

Colbeck, S.C. (1983). Theory of metamorphism of dry snow. Journal of Geophysical Research, 88 (C9), 5475-5482.

Colbeck, S.C. (1987). History of snow-cover research. Journal of Glaciology, Special Issue, 60-65.

Colbeck, S.C. (1989). Snow-crystal growth with varying surface temperatures and radiation penetration. Journal of Glaciology, 35 (119), 23-29.

Colbeck, S.C. (1991). The layered character of snow covers. Reviews of Geophysics, 29 (1), 81-96.

Colbeck, S.C. (1993). The vapor diffusion coefficient for snow. Water Resources Research, 29 (1), 109-115.

Delaney, L.J., Houston, R.W., & Eagleton, L.C. (1964). The rate of vaporization of water and ice. Chemical Engineering Science, 19, 105-114.

de Quervain, M.R. (1963). On the metamorphosis of snow. In W.D. Kingery (Ed.), Ice and Snow (pp. 377-390). Cambridge, MA: The M.I.T. Press.

Dorsey, N.E. (Comp.) (1968). Properties of Ordinary Water-Substance. New York: Hafner.

Fukusako, S. (1990). Thermophysical properties of ice, snow, and sea ice. International Journal of Thermophysics, 11 (2), 353-372.

Gubler, H. (1985). Model for dry snow metamorphism by interparticle vapor flux. Journal of Geophysical Research, 90 (D5), 8081-8092.

Hansen, A.C. & Brown, R.L. (1986). The granular structure of snow: an internal-state variable approach. Journal of Glaciology, 32 (112), 434-438.

Hansen, A.C. (1989). Reexamining some basic definitions of modern mixture theory. International Journal of Engineering Science, 27 (12), 1531-1534.

Hansen, A.C., Crane, R.L., Damson, M.H., Donovan, R.P., Horning, D.T., & Walker, J.L. (1991). Some notes on a volume fraction mixture theory and a comparison with the kinetic theory of gases. International Journal of Engineering Science, 29 (5), 561-573.

Hansen, A.C., Walker, J.L., & Donovan, R.P. (1994). A finite element formulation for composite structures based on a volume fraction mixture theory. International Journal of Engineering Science, 32 (1), 1-17.

Hobbs, P.V. (1974). Ice Physics. Oxford: Clarendon Press.

Incropera, F.P. & DeWitt, D.P. (1985). Fundamentals of Heat and Mass Transfer. 2nd Edition. New York: John Wiley & Sons.

McComb, T.J.L., Rimmer, A.B., Rodgers, M.L.B., Turver, K.E., & Vickers, A.F. (1992). A mathematical model for the prediction of temperature in a dry snow layer. Cold Regions Science and Technology, 20, 247-259.

Marbouty, D. (1980). An experimental study of temperature-gradient metamorphism. Journal of Glaciology, 26 (94), 303-312.

Nield, D.A. & Bejan, A. (1992). Convection in porous media. New York: Spring-Verlag.

Passman, S.L., Nunziato, J.W., & Walsh, E.K. (1984). A theory of multiphase mixtures. In C. Truesdell (Comp.), Rational Thermodynamics (pp. 286-325). New York: McGraw-Hill.

Sommerfeld, R.A. & LaChapelle, E. (1970). The classification of snow metamorphism. Journal of Glaciology, 9 (55), 3-17.

Truesdell, C. (1984). Rational Thermodynamics. New York: McGraw-Hill.

Underwood, E.E. (1970). Quantitative Stereology. Reading, MA: Addison-Wesley.

APPENDIX A

```
      PROGRAM MAIN
*
*     AUTHOR:  WAYNE E. FOSLIEN
*     DATE:  JULY 1994
*
*     PROGRAM DESCRIPTION:
*       THIS FORTRAN PROGRAM IS A FINITE ELEMENT BASED PROGRAM
*       THAT CAN BE USED TO SOLVE THE GENERAL STURM-LIOUVILLE
*       PROBLEM WITH A TIME DERIVATIVE TERM.  A CRANK-NICHOLSON
*       TIME INTEGRATION SCHEME IS USED TO MARCH FORWARD IN TIME.
*       THE CODE THAT FOLLOWS SPECIFICALLY SOLVES THE NONLINEAR
*       EQUATIONS GOVERNING HEAT AND MASS TRANSFER IN SNOW BY A
*       SIMPLE ITERATIVE TECHNIQUE.
*
*     VARIABLE DESCRIPTION:
*       T = TIME
*       TOUT = TIME TO OUTPUT DATA
*       TMAX = UPPER TIME LIMIT FOR INTEGRATION
*       H = TIME STEP
*       K = COUNTER FOR COEFFICIENT MATRIX UPDATE
*       CHATO = PREVIOUS TIME STEP VALUE OF MASS SUPPLY
*       CHAT = CURRENT TIME STEP'S VALUE OF MASS SUPPLY
*       ERR = CHANGE IN SOLUTION FROM PREVIOUS ITERATION
*             BASED ON L2 NORM
*       TOL = TOLERANCE ON THE ERROR IN THE SOLUTION
*       TEMP = TEMPERATURE OF SNOW AT CURRENT TIME STEP
*       TEMPP = TEMPERATURE OF SNOW AT PREVIOUS ITERATION
*       IT = NUMBER OF ITERATIONS
*       ITMAX = MAXIMUM NUMBER OF ITERATIONS ALLOWED

      IMPLICIT DOUBLE PRECISION (A-H,O-Z)
      IMPLICIT INTEGER (I-N)

      INCLUDE 'COMMON.F'

      OPEN (UNIT=10, FILE='ELEM.DAT',STATUS='OLD')
      OPEN (UNIT=15, FILE='ICBC.DAT',STATUS='OLD')
      OPEN (UNIT=16, FILE='PHIO.DAT',STATUS='OLD')
      OPEN (UNIT=20, FILE='ECHO.DAT',STATUS='UNKNOWN')
      OPEN (UNIT=30,FILE='TEMP.dat',STATUS='UNKNOWN')
      OPEN (UNIT=35,FILE='DTDX.DAT',STATUS='UNKNOWN')

      CALL INPUT

      T=H
      K=0
      CALL INITIALIZE
      DO 10 I=1,NPOIN
        CHATO(I)=0.0D0
 10   CONTINUE

 20   CALL TEMPIV
```

```
*
*  CHECK FOR CONVERGENCE AT CURRENT TIME STEP
*
      ERR=0.0D0
      DO 40 I=1,NPOIN
        ERR=ERR+(TEMP(I)-TEMPP(I))**2.
*        print *, 'temp=',temp(i),tempp(i)
 40   CONTINUE
      ERR = SQRT(ERR)
*      PRINT *, 'ERR=',ERR
      IF (ERR.LE.TOL) THEN
        CALL PHI
*        ERRSS=0.0D0
*        DO 42 I=1,NPOIN
*          ERRSS=ERRSS+DABS(TEMP(I)-TEMPO(I))
* 42     CONTINUE
*        PRINT *, 'ERRSS=',ERRSS
*        IF (ERRSS.LT.TOL*1.D5) THEN
*          CALL OUTPUT (1)
*          STOP
*        ENDIF
        IF (T.EQ.TOUT) THEN
          CALL OUTPUT(0)
          TOUT=TOUT+86400.D0
        ENDIF
*        PRINT *, 'TIME=',T
        T=T+H
        IT=0
        K=K+1
*
*  STORE CURRENT CONVERGED SOLUTION
*
        DO 45 I=1,NPOIN
*          print *, 'temp=',temp(i)
          TEMPO(I)=TEMP(I)
          TEMPP(I)=TEMPO(I)
          CHATO(I)=CHAT(I)
          RLOAD(I)=0.0D0
 45     CONTINUE
      ELSE
        IF (K.EQ.0) K=K+1
        IF (IT.EQ.ITMAX) THEN
          PRINT *, 'IT=',IT,'T=',T
          STOP
        ENDIF
        IT=IT+1
*        print *, 'it=',it
        DO 47 I=1,NPOIN
          TEMPP(I)=TEMP(I)
          RLOAD(I)=0.0D0
 47     CONTINUE
        GOTO 20
      ENDIF

      IF (K.EQ.KMAX) THEN
        K=0
```

```
        CALL INITIALIZE
      ENDIF

      IF (T.LE.TMAX) GOTO 20

      END

*************************************************

      SUBROUTINE INITIALIZE

*     SUBROUTINE DESCRIPTION:
*       INITIALIZE ALL VARIABLES FROM INTEG SUBROUTINE
*
      IMPLICIT DOUBLE PRECISION (A-H,O-Z)
      IMPLICIT INTEGER (I-N)

      INCLUDE 'COMMON.F'

      DO 25 I=1,NPOIN
      DO 23 J=1,NPOIN
        STIFF(I,J)=0.0D0
        STR(I,J)=0.0D0
 23   CONTINUE
 25   CONTINUE
      DO 28 I=1,3
        FLOAD(I)=0.0D0
      DO 27 J=1,3
        SMR(I,J)=0.0D0
        SK(I,J)=0.0D0
        SM(I,J)=0.0D0
        SRR(I,J)=0.0D0
 27   CONTINUE
 28   CONTINUE

      RETURN
      END

*************************************************************

      DOUBLE PRECISION FUNCTION GS(TE)

      IMPLICIT DOUBLE PRECISION (A-H), DOUBLE PRECISION (O-Z)
      IMPLICIT INTEGER (I-N)

*
*     PURPOSE:
*       CALCULATE THE VAPOR DENSITY OF WATER
*
*     VARIABLES:
*       TE = TEMPERATURE
*       C* = CONSTANTS USED TO CALCULATE DENSITY
*       RV = GAS CONSTANT FOR WATER VAPOR
*

      DATA C1,C2,C3/-2445.5646D0,8.2312D0,-1.677006D-2/
```

```
      DATA C4,C5/1.20514D-5,-6.757169D0/
      DATA C6,RV/133.3224D0,461.9D0/

      GS=(10.D0**(C1/TE+C2*DLOG10(TE)+C3*TE+C4*TE*TE+C5))*C6/RV/TE

      RETURN
      END

*****************************************************************

      DOUBLE PRECISION FUNCTION DDGDT(TE)

*     PURPOSE:
*       THIS SUBROUTINE CALCULATES THE SECOND DERIVATIVE OF
*       THE DENSITY WITH RESPECT TO THE TEMPERATURE.
*
*     VARIABLE DESCRIPTION:
*       TE = TEMPERATURE

      IMPLICIT DOUBLE PRECISION (A-H,O-Z), INTEGER (I-N)

      DATA C1,C2,C3,C4/-2445.5646D0,8.2312D0,-1.677006D-2,1.20514D-5/

      DDGDT=DGDT(TE)*DLOG(10.D0)*(-C1/TE**2+(C2-1.D0)/TE/DLOG(10.D0)
     & +C3+2.D0*C4*TE)+GS(TE)*DLOG(10.D0)*(2.D0*C1/TE**3+(1.D0-C2)/
     & TE**2/DLOG(10.D0)+2.D0*C4)

      RETURN
      END

*****************************************************

      DOUBLE PRECISION FUNCTION DGDT(TE)

*     PURPOSE:
*       THIS SUBROUTINE CALCULATES THE FIRST DERIVATIVE
*       OF THE DENSITY WITH RESPECT TO THE TEMPERATURE.
*
*     VARIABLE DESCRIPTION:
*       TE = TEMPERATURE

      IMPLICIT DOUBLE PRECISION (A-H,O-Z), INTEGER (I-N)
      DATA C1,C2,C3,C4/-2445.5646D0,8.2312D0,-1.677006D-2,1.20514D-5/

      DGDT=GS(TE)*DLOG(10.D0)*(-C1/TE**2+(C2-1.D0)/TE/DLOG(10.D0)+C3
     &     +2.D0*C4*TE)

      RETURN
      END

*****************************************************

      SUBROUTINE PHI

*     PURPOSE:
*       INTEGRATE THE VOLUME FRACTION OF ICE
```

```
*
*     VARIABLE DESCRIPTION:
*       H = TIME STEP
*       CHAT = MASS SUPPLY
*       GI = DENSITY OF ICE
*       PHIIO = PREVIOUS TIME STEP VALUE FOR THE VOLUME
*               FRACTION OF ICE
*       PHII = NEW VALUE FOR THE VOLUME FRACTION OF ICE

      IMPLICIT DOUBLE PRECISION (A-H,O-Z)
      IMPLICIT INTEGER (I-N)

      INCLUDE 'COMMON.F'

      DO 10 I=1,NPOIN
        PHII(I)=H*CHAT(I)/GI + PHIIO(I)
*        print *, 'phii=',phii(i)
 10   CONTINUE

      RETURN
      END

************************************************

      SUBROUTINE TEMPIV

*     PURPOSE:
*       CALCULATE THE COEFFICIENTS TO THE DIFFERENTIAL EQUATION
*       AND CALL THE SUBROUTINE TO INTEGRATE.
*
*     VARIABLE DESCRIPTION:
*       F = FORCING FUNCTION TERM IN DE
*       P = SPATIAL DERIVATIVE COEFFICIENT IN DE
*       Q = DEPENDENT VARIABLE COEFFICIENT IN DE
*       AMN = TIME DERIVATIVE COEFFICIENT IN DE
*       TCI = THERMAL CONDUCTIVITY OF ICE
*       TCA = THERMAL CONDUCTIVITY OF AIR
*       GI = DENSITY OF ICE
*       PHIV = VOLUME FRACTION OF VAPOR
*       PHII = VOLUME FRACTION OF ICE
*       CVA = SPECIFIC HEAT OF AIR AT CONSTANT VOLUME
*       CVI = SPECIFIC HEAT OF ICE AT CONSTANT VOLUME
*       TEMPO = PREVIOUS TIME STEP TEMPERATURE
*       USG = INTERNAL ENERGY LATENT HEAT
*

      IMPLICIT DOUBLE PRECISION (A-H,O-Z)
      IMPLICIT INTEGER (I-N)

      INCLUDE 'COMMON.F'

      DIMENSION F(NPOIN),P(NPOIN),Q(NPOIN),AMN(NPOIN)

      CALL MASSUPLY

      DO 10 I=1,NPOIN
```

```
        IF (K.EQ.0.OR.K.EQ.KMAX) P(I)=TSNOW(I)
        IF (K.EQ.0.OR.K.EQ.KMAX) AMN(I)=PHII(I)*GI*CVI+PHIV(PHII(I))
     &                                  *GA*CVA
        F(I)=USG(263.15D0)*CHATO(I)+USG(263.15D0)*CHAT(I)
        Q(I)=0.0D0
 10   CONTINUE

      CALL INTEG(F,P,Q,AMN,TEMPO,TEMP)

      RETURN
      END

*******************************************************

      DOUBLE PRECISION FUNCTION TSNOW (I)

*     PURPOSE:
*       CALCULATE THE EFFECTIVE THERMAL CONDUCTIVITY OF SNOW DUE TO
*       CONDUCTION ALONE.

      IMPLICIT DOUBLE PRECISION (A-H,O-Z)
      IMPLICIT INTEGER (I-N)

      INCLUDE 'COMMON.F'

      TSNOW = PHII(I)*TPORE(I) + (1.D0-PHII(I))*TLAM(I)

      RETURN
      END

*******************************************************

      DOUBLE PRECISION FUNCTION TPORE(I)

*     PURPOSE:
*       CALCULATE THE THERMAL CONDUCTIVITY OF THE PORE MICROSTRUCTURE
*
      IMPLICIT DOUBLE PRECISION (A-H,O-Z)
      IMPLICIT INTEGER (I-N)

      INCLUDE 'COMMON.F'

      TPORE = PHII(I)*TCI(TEMP(I)) + (1.D0-PHII(I))*
     &        TCA(TEMP(I)+273.15D0)

      RETURN
      END

*******************************************************

      DOUBLE PRECISION FUNCTION TCI(TE)

      IMPLICIT DOUBLE PRECISION (A-H,O-Z)
      IMPLICIT INTEGER (I-N)

*
```

```
*     EXPERIMENTAL CORRELATION BELOW FROM FUKUSAKO (1990)
*     VALID FOR -173 C - 0 C

      TCI = 1.16D0*(1.91D0-8.66D-3*TE+2.97D-5*TE**2.D0)

      RETURN
      END

*******************************************************

      DOUBLE PRECISION FUNCTION TCA (TE)

      IMPLICIT DOUBLE PRECISION (A-H,O-Z)
      IMPLICIT INTEGER (I-N)

*
*     LINEAR BEST FIT LINE BELOW FROM DATA IN INCROPERA & DEWITT (1985)
*     FOR TEMPERATURES 250K - 300K

      TCA = 8.D-5*(TE-250.D0)+0.0223D0

      RETURN
      END

*******************************************************

      DOUBLE PRECISION FUNCTION TLAM(I)

*
*     PURPOSE:
*       CALCULATE THE THERMAL CONDUCTIVITY OF THE LAMELLAE
*       MICROSTRUCTURE.

      IMPLICIT DOUBLE PRECISION (A-H,O-Z)
      IMPLICIT INTEGER (I-N)

      INCLUDE 'COMMON.F'

      TCAC=TCA(TEMP(I)+273.15D0)
      TCIC=TCI(TEMP(I))
      TLAM = TCAC*TCIC/(PHII(I)*(TCAC+USG(263.15D0)*DV(TEMP(I)
     &       +273.15)*DGDT(TEMP(I)+273.15))+(1.D0-PHII(I))*TCIC)

      RETURN
      END

*******************************************************

      SUBROUTINE MASSUPLY

      IMPLICIT DOUBLE PRECISION (A-H,O-Z)
      IMPLICIT INTEGER (I-N)

      INCLUDE 'COMMON.F'

*     PURPOSE:
```

```
*       CALCULATE THE MASS SUPPLY CHAT
*
*     VARIABLE DESCRIPTION:
*       VJ = MASS FLUX OF VAPOR
*       DTDT = RATE OF CHANGE OF VAPOR DENSITY WITH TIME TIMES PHIV
*       DTDX = FIRST SPATIAL DERIVATIVE OF TEMPERATURE
*       DX = SPATIAL STEP
*       DEFF = EFFECTIVE DIFFUSION COEFFICIENT OF WATER VAPOR IN SNOW
*
      DO 10 I=1,NPOIN
        IF (I.EQ.1) THEN
          DTDX(I)=(-3.D0*TEMP(1)+4.D0*TEMP(2)-TEMP(3))/2.D0/DX
        ELSEIF (I.EQ.NPOIN) THEN
          DTDX(I)=(3.D0*TEMP(I)-4.D0*TEMP(I-1)+TEMP(I-2))/2.D0/DX
        ELSE
          DTDX(I)=(TEMP(I+1)-TEMP(I-1))/2.D0/DX
        ENDIF
        VJ(I)=-DEFF(I)*DGDT(TEMP(I)+273.15D0)
     &          *DTDX(I)
*         PRINT *, 'VJ=',VJ(I),I
*         PRINT *, 'CHAT=',CHAT(I) ,I
 10   CONTINUE
      DO 20 I=1,NPOIN
        DTDT=PHIV(PHII(I))*DGDT(TEMP(I)+273.15)*(TEMP(I)-TEMPO(I))/H
        IF (I.EQ.1) THEN
          CHAT(I)=-(-3.D0*VJ(I)+4.D0*VJ(I+1)-VJ(I+2))/2.D0/DX-DTDT
*          CHAT(I)=-VJ(I)/DX
        ELSEIF (I.EQ.NPOIN) THEN
          CHAT(I)=-(3.D0*VJ(I)-4.D0*VJ(I-1)+VJ(I-2))/2.D0/DX-DTDT
        ELSE
          CHAT(I)=-(VJ(I+1)-VJ(I-1))/2.D0/DX-DTDT
        ENDIF
*         PRINT *, 'CHAT=',CHAT(I),I
 20   CONTINUE

      RETURN
      END

*******************************************************

      DOUBLE PRECISION FUNCTION DEFF(I)

*     PURPOSE:
*       CALCULATE THE EFFECTIVE DIFFUSION COEFFICIENT FOR SNOW

      IMPLICIT DOUBLE PRECISION (A-H,O-Z)
      IMPLICIT INTEGER (I-N)

      INCLUDE 'COMMON.F'

      D = DV(TEMP(I)+273.15D0)
      TCIC=TCI(TEMP(I))
      TCAC=TCA(TEMP(I)+273.15D0)
      DEFF=(PHII(I)*PHIV(PHII(I))+PHIV(PHII(I))*TCIC/(PHII(I)*
     &     (TCAC+USG(263.15D0)*D*DGDT(TEMP(I)+273.15D0))+PHIV(PHII(I))*
     &     TCIC))*D
```

```
      RETURN
      END

*************************************************************

      DOUBLE PRECISION FUNCTION DV(TE)
      IMPLICIT DOUBLE PRECISION (A-H), DOUBLE PRECISION (O-Z)
      IMPLICIT INTEGER (I-N)

*
*     PURPOSE:
*       CALCULATE THE CORRECTION ON THE WATER VAPOR DIFFUSIVITY
*       IN AIR DUE TO TEMPERATURE CHANGES.
*
*     VARIABLES:
*       DO = WATER VAPOR DIFFUSIVITY AT TO
*       TO = REFERENCE TEMPERATURE FOR DO
*       TE = TEMPERATURE
*
      DATA DO,TO/0.26D-4,298.0D0/

      DV = DO*(TE/TO)**1.5D0

      RETURN
      END

*****************************************************

      DOUBLE PRECISION FUNCTION PHIV(PHII)

      IMPLICIT DOUBLE PRECISION (A-H,O-Z)
      IMPLICIT INTEGER (I-N)

*C
*C     PURPOSE:
*C       CALCULATE THE VOLUME FRACTION OF THE VAPOR GIVEN THE VOLUME
FRACTION OF THE
*C       ICE
*C
*C     VARIABLES:
*C       PHII = VOLUME FRACTION OF ICE
*C       PHIV = VOLUME FRACTION OF VAPOR
*C
*
      PHIV=1.D0-PHII
      RETURN
      END

*****************************************************

      DOUBLE PRECISION FUNCTION USG(TE)

      IMPLICIT DOUBLE PRECISION (A-H,O-Z)
      IMPLICIT INTEGER (I-N)
```

```
*
*  THIS FUNCTION CALCULATES THE INTERNAL ENERGY CHANGE DUE TO PHASE
CHANGE
*  FROM ICE TO WATER VAPOR
*
      USG=(2626.11D0+1.31763D0*TE-3.71584D-3*TE**2)*1.D3

      RETURN
      END


**********************************************************************
******
*                     SUBROUTINE INPUT
*
**********************************************************************
******
      SUBROUTINE INPUT

      IMPLICIT DOUBLE PRECISION (A-H,O-Z)
      IMPLICIT INTEGER (I-N)
      INCLUDE 'COMMON.F'
*C
*C     CALLED BY: SANDL
*C     CALLS    : NONE
*C
      CHARACTER *40  TITLE
*C
*C---->READ THE TITLE
*C
      READ(10,1000) TITLE

*C
*C---->READ THE GRID CONTROL DATA
*C
      READ(10,1015) IWRITE, KMAX
*      NPOIN = 2*NELEM+1

        READ(10,1060) X(1)
        READ(10,1060) X(NPOIN)


      DX = (X(NPOIN)-X(1))/DBLE(FLOAT(NPOIN-1))
      DO 20 I=2,NPOIN-1
      X(I)=X(I-1)+DX
      PRINT *, 'X=',X(I)
 20   CONTINUE
*C
*C---->DEVELOP THE ELEMENT CONNECTIVITY ARRAY
*C
      DO 40 IELEM = 1, NELEM
      DO 30 INODE=1, 3
        LNODE(IELEM,INODE)=2*IELEM-1 + (INODE-1)
 30   CONTINUE

   40 CONTINUE
```

```
*C
*C     READ THE TIME STEP VALUE
*C
      READ (10,1060) H
      PRINT *, 'H=',H
      READ (10,1060) TMAX

      READ (10,1060) TOL
      READ (10,1060) TOUT
      READ (10,900) ITMAX


**********************************************************************
*C
*C---->READ THE INITIAL CONDITION AND BOUNDARY CONDITION DATA
*C

      DO 100 I=1,2
      GOTO (70,90) I

 70   READ (15,1060) TEMPO(1)
      PRINT *, 'TEMPO=',TEMPO(1)
      DO 75 J=1,NPOIN
        TEMPO(J)=TEMPO(1)
        TEMPP(J)=TEMPO(1)
        TEMP(J)=TEMPO(1)
 75   CONTINUE
      GOTO 95

 90   DO 92 J=1,NPOIN
        READ (16,1070) PHIIO(J)
        PHII(J)=PHIIO(J)
        PRINT *,PHII(J)
 92   CONTINUE
      GOTO 100


 95   READ (15,1040) NA,NB
        IF (NA .EQ. 1) THEN
          READ(15,1050) AA, ALPHA

        ELSE
          READ(15,1060) UA

        END IF
        IF (NB .EQ. 1) THEN
          READ(15,1050) BB, BETA

        ELSE
          READ(15,1060) UB

        ENDIF
 100   CONTINUE
      IF (NA.EQ.2) TEMPP(1)=UA
      IF (NB.EQ.2) TEMPP(NPOIN)=UB
*C
```

```
*C---->FORMAT STATEMENTS FOR INPUT
*C
  900 FORMAT(10X,I5)
 1000 FORMAT(10X, A30)
 1010 FORMAT(10X, 2I5)
 1015 FORMAT(10X, I5,I10)
 1020 FORMAT(10X, I5, 5X, G10.4)
 1030 FORMAT(10X, 4(I5,5X))
 1040 FORMAT(10X, I5, I5)
 1050 FORMAT(10X, 2G10.4)
 1060 FORMAT(10X, G10.4)
 1070 FORMAT(5X,G10.4)
*C
*CCCCCCCCCCCCCCCCCCCCC
*C
*C---->ECHO THE INPUT
*CCCCCCCCCCCCCCCCCCCCCC
      WRITE(20,2000)
      WRITE(20,2010) TITLE
      WRITE(20,2020)
*
*
*     ECHO ALL INPUT
*
***********************************
      WRITE (20,2030) NELEM,NPOIN
      WRITE (20,2035) H
      WRITE (20,2036) TMAX
      WRITE (20,2040)
      DO 120 I=1,NPOIN
        WRITE (20,2050) I,X(I),TEMPO(I),PHIIO(I)
 120   CONTINUE
       WRITE (20,2061)
        IF (NA.EQ.1) THEN
          WRITE (20,2070) AA,ALPHA
        ENDIF
        IF (NB.EQ.1) THEN
          WRITE (20,2075) BB,BETA
        ENDIF
        IF (NA.EQ.2) THEN
            WRITE (20,2080) UA
        ENDIF
        IF (NB.EQ.2) THEN
          WRITE (20,2085) UB
        ENDIF
 180  CONTINUE
 2000 FORMAT(21X,'UW-ME533',//,115X,'1-D FINITE ELEMENT ANALYSIS',////)
 2010 FORMAT(3X,A40,//)
 2020 FORMAT(1X,26('*'),2X,'ECHOED INPUT',2X,26('*'))
 2030 FORMAT(2X,'NUMBER OF ELEMENTS= ',I5,' NUMBER OF POINTS IN DOMAIN='
     &       1X,I5)
 2035 FORMAT(2X,'THE TIME STEP= ',F7.3)
 2036 FORMAT (2X,'THE INTEGRATION DURATION IS TMAX= ',F7.3)
 2040 FORMAT('POINT NO.',6X,'X',7X,'TVO',7X,'TIO',7X,'GVO',7X,'PHIIO')
 2050 FORMAT(I5,5X,5(F7.3,3X))
 2060 FORMAT('BOUNDARY CONDITIONS FOR VAPOR TEMPERATURE:')
```

```
 2061 FORMAT('BOUNDARY CONDITIONS FOR ICE TEMPERATURE:')
 2062 FORMAT('BOUNDARY CONDITIONS FOR VAPOR DENSITY:')
 2063 FORMAT(1x,'ICE VOLUME FRACTION DOESNT REQUIRE BOUNDARY
     &        CONDITIONS.')
 2070 FORMAT('NATURAL:',2X,'A= ',F7.3,2X,'ALPHA= ',F7.3)
 2075 FORMAT('NATURAL:',2X,'B= ',F7.3,2X,'BETA= ',F7.3)
 2080 FORMAT('ESSENTIAL:',2X,'UA= ',F7.3)
 2085 FORMAT('ESSENTIAL:',2X,'UB= ',F7.3)
      RETURN
      END

*****************************************************************

      SUBROUTINE OUTPUT (ISS)

      IMPLICIT DOUBLE PRECISION (A-H,O-Z)
      IMPLICIT INTEGER (I-N)

      INCLUDE 'COMMON.F'

      IF (ISS.EQ.0) THEN
        WRITE (30,*) T
        DO 45 I=1,NPOIN
          PRINT *, X(I), TEMP(I), PHII(I)
          WRITE (30,1000) X(I),TEMP(I),PHII(I),CHAT(I)
          WRITE (35,1010) X(I),DTDX(I)
*          WRITE (55,*) X(I),PHII(I)
 45     CONTINUE
      ELSE
        WRITE (31,*) T
        DO 50 I=1,NPOIN
          WRITE (31,1020) X(I), TEMP(I), PHII(I),CHAT(I),VJ(I)

 50     CONTINUE
      ENDIF
 1000 FORMAT (E12.4,1X,E12.4,1X,E12.4,1X,E12.4)
 1010 FORMAT (E12.4,1XE12.4)
 1020 FORMAT (E12.4,1X,E12.4,1X,E12.4,1X,E12.4,1X,E12.4)
      RETURN
      END

*************************************************************

      SUBROUTINE INTEG (F,P,Q,AMN,UO,U)

      IMPLICIT DOUBLE PRECISION (A-H,O-Z)
      IMPLICIT INTEGER (I-N)

      INCLUDE 'COMMON.F'

      DIMENSION U(NPOIN),UO(NPOIN),AMN(NPOIN),F(NPOIN),P(NPOIN)
      DIMENSION Q(NPOIN),RHS(NPOIN)
      DIMENSION INDX(NPOIN),VV(NPOIN)

      DO 10 I=1,NPOIN
        RLOAD(I)=0.0D0
```

```
 10   CONTINUE

      DO 50 IELEM = 1, NELEM
         IF (K.EQ.0.OR.K.EQ.KMAX) CALL FORMSMR(IELEM,P,Q,AMN)
       CALL FORMLOAD(IELEM,F)
         IF( IWRITE .EQ. 2 ) CALL OUT(1,IELEM)
         CALL INDEX(IELEM)
         IF (K.EQ.0.OR.K.EQ.KMAX) CALL ASSEMBLES
       CALL ASSEMBLEL
         IF( IWRITE .EQ. 2 ) CALL OUT(2,IELEM)
   50 CONTINUE
*      print *, 'k=',k
      DO 55 I=1,NPOIN
        RHS(I)=0.0D0
        DO 57 J=1,NPOIN
          RHS(I)=STR(I,J)*UO(J)+RHS(I)
 57     CONTINUE
      RLOAD(I)=RLOAD(I)+RHS(I)
 55   CONTINUE

      IF (K.EQ.0.OR.K.EQ.KMAX) CALL BOUNDS
*      print *, 'ks=',k
      CALL BOUNDL
*      print *, 'kl=',k
*      IF( IWRITE .EQ. 2 ) CALL OUT(2, NELEM)
*      IF( IWRITE .EQ. 2 ) CALL OUT(3, NELEM)

*      DO 59 I=1,NPOIN
*      DO 58 J=1,NPOIN
*        A(I,J)=STIFF(I,J)
* 58   CONTINUE
*      INDX(I)=IN(I,IBC)
* 59   CONTINUE

      IF (K.EQ.0.OR.K.EQ.KMAX) THEN
      PRINT *, 'GOING TO LUDCMP'
        CALL LUDCMP(STIFF, VV, INDX, NPOIN, D)
*        DO 70 I=1,NPOIN
*        DO 60 J=1,NPOIN
*          STIFF(I,J)=A(I,J)
* 60     CONTINUE
*          IN(I,IBC)=INDX(I)
* 70     CONTINUE
      ENDIF
*      IF (K.NE.0.AND.K.NE.KMAX) THEN
*        DO 85 I=1,NPOIN
*        INDX(I)=IN(I,IBC)
*      DO 80 J=1,NPOIN
*        A(I,J)=STIFF(I,J,IBC)
* 80     CONTINUE
* 85   CONTINUE
*      ENDIF
*      print *, 'going to lubksb'
      CALL LUBKSB(STIFF,INDX,NPOIN,RLOAD)

*
```

```
* COPY THE RESULTS FROM RLOAD(I) INTO U(I)
*
      DO 90 I= 1, NPOIN
        U(I) = RLOAD(I)
   90 CONTINUE

      RETURN
      END

**********************************************************************
******
*                     SUBROUTINE OUTPUT OF STIFFNESS MATRIX COMPONENTS
*
**********************************************************************
******

      SUBROUTINE OUT (ICODE,NM)

      IMPLICIT DOUBLE PRECISION (A-H,O-Z)
      IMPLICIT INTEGER (I-N)

      INCLUDE 'COMMON.F'

      GO TO (100,200,300,400) ICODE

  100 WRITE(40,600) NM
  600 FORMAT(1H1,//,10X,'ELEMENT STIFFNESS MATRIX, MEM. NO.',I3,/)
      WRITE(40,601)((SMR(I,J),J=1,3),I=1,3)
  601 FORMAT(10X,4E14.7)
      RETURN

  200 WRITE(40,602) NM
  602 FORMAT(//,10X,'GLOBAL STIFFNESS MATRIX: MEMBERS 1 THRU. ',I2)
      DO 49 I = 1, NPOIN
*         DO 48 J = 1, NPOIN
*   48       WRITE(40,809) I,J,STIFF(I,J,IBC)
  809       FORMAT(I3,I3,E12.5)
            WRITE(40,603)
  603       FORMAT(//)
   49 CONTINUE
      RETURN

  300 WRITE(40,810)
  810 FORMAT(1H1,//,10X,'LOAD VECTOR')
      WRITE(40,811) (RLOAD(I) , I=1, NPOIN)
  811 FORMAT(10X,E14.7)
      RETURN

*  400 IJT = 0
  400    WRITE (40,*) 'RESULTS:   NODE                    U'
      DO 79 IPOIN = 1, NPOIN
*         WRITE(40,813) IPOIN, U(IPOIN)
  813    FORMAT(10X,I3,13X,G12.5)
  79  CONTINUE
      RETURN
      END
```

```
************************************************************
*                      SUBROUTINE FORMSMR                  *
************************************************************
      SUBROUTINE FORMSMR(IELEM,P,Q,AMN)

      IMPLICIT DOUBLE PRECISION (A-H,O-Z)
      IMPLICIT INTEGER (I-N)

      INCLUDE 'COMMON.F'

      DIMENSION AMN(NPOIN),P(NPOIN),Q(NPOIN)

*
*   THIS ROUTINE FORMS THE LOCAL ELEMENT STIFFNESS MATRIX
*



*
*   DETERMINE WHAT THE NODE NUMBER I IS AT THE LEFT END OF EACH ELEMENT
*
       I=LNODE(IELEM,1)
*
*   DETERMINE THE ELEMENT LENGTH, EL, BASED ON NODAL VALUES
*
      EL=X(I+2)-X(I)
*
*   CALCULATE THE LOCAL STIFFNESS MATRIX BY CALLING SPECIAL INTEGRATION
*   FUNCTIONS
*
      SK(1,1)=PE(37.D0,36.D0,-3.D0,I,EL,P)+QE(39.D0,20.D0,-3.D0,I,EL,Q)
      SK(1,2)=PE(-44.D0,-32.D0,-4.D0,I,EL,P)
     &        +QE(20.D0,16.D0,-8.D0,I,EL,Q)
      SK(1,3)=PE(7.D0,-4.D0,7.D0,I,EL,P)+QE(-3.D0,-8.D0,-3.D0,I,EL,Q)
      SK(2,2)=PE(48.D0,64.D0,48.D0,I,EL,P)+QE(16.D0,192.D0,16.D0,I,EL,Q)
      SK(2,3)=PE(-4.D0,-32.D0,-44.D0,I,EL,P)
     &        +QE(-8.D0,16.D0,20.D0,I,EL,Q)
      SK(3,3)=PE(-3.D0,36.D0,37.D0,I,EL,P)+QE(-3.D0,20.D0,39.D0,I,EL,Q)

      SM(1,1)=QE(39.D0,20.D0,-3.D0,I,EL,AMN)
      SM(1,2)=QE(20.D0,16.D0,-8.D0,I,EL,AMN)
      SM(1,3)=QE(-3.D0,-8.D0,-3.D0,I,EL,AMN)
      SM(2,2)=QE(16.D0,192.D0,16.D0,I,EL,AMN)
      SM(2,3)=QE(-8.D0,16.D0,20.D0,I,EL,AMN)
      SM(3,3)=QE(-3.D0,20.D0,39.D0,I,EL,AMN)

      SMR(1,1)=H/2.D0*SK(1,1)+SM(1,1)
      SMR(1,2)=H/2.D0*SK(1,2)+SM(1,2)
      SMR(1,3)=H/2.D0*SK(1,3)+SM(1,3)
      SMR(2,2)=H/2.D0*SK(2,2)+SM(2,2)
      SMR(2,3)=H/2.D0*SK(2,3)+SM(2,3)
      SMR(3,3)=H/2.D0*SK(3,3)+SM(3,3)

      SRR(1,1)=-H/2.D0*SK(1,1)+SM(1,1)
      SRR(1,2)=-H/2.D0*SK(1,2)+SM(1,2)
      SRR(1,3)=-H/2.D0*SK(1,3)+SM(1,3)
```

```
      SRR(2,2)=-H/2.D0*SK(2,2)+SM(2,2)
      SRR(2,3)=-H/2.D0*SK(2,3)+SM(2,3)
      SRR(3,3)=-H/2.D0*SK(3,3)+SM(3,3)

*
*  THE STIFFNESS MATRIX IS SYMMETRIC FOR STURM-LIOUVILLE PROBLEMS
*  SO SET THE LOWER TRIANGLE OF THE COEFFICIENTS EQUAL TO ITS
CORRESPONDING
*  VALUE IN UPPER TRIANGLE
*
      SMR(2,1)=SMR(1,2)
      SMR(3,1)=SMR(1,3)
      SMR(3,2)=SMR(2,3)

      SRR(2,1)=SRR(1,2)
      SRR(3,1)=SRR(1,3)
      SRR(3,2)=SRR(2,3)

      RETURN
      END

************************************************************

      SUBROUTINE FORMLOAD (IELEM,F)
      IMPLICIT DOUBLE PRECISION (A-H,O-Z)
      IMPLICIT INTEGER (I-N)
      INCLUDE 'COMMON.F'
      DIMENSION F(NPOIN)

*
*  DETERMINE WHAT THE NODE NUMBER I IS AT THE LEFT END OF EACH ELEMENT
*
       I=LNODE(IELEM,1)
*
*  DETERMINE THE ELEMENT LENGTH, EL, BASED ON NODAL VALUES
*
      EL=X(I+2)-X(I)

      FLOAD(1)=H/2.D0*FE(4.D0,2.D0,-1.D0,I,EL,F)
      FLOAD(2)=H/2.D0*FE(2.D0,16.D0,2.D0,I,EL,F)
      FLOAD(3)=H/2.D0*FE(-1.D0,2.D0,4.D0,I,EL,F)

      RETURN
      END

************************************************************

      DOUBLE PRECISION FUNCTION PE(C1,C2,C3,I,EL,P)

      IMPLICIT DOUBLE PRECISION (A-H,O-Z)
      IMPLICIT INTEGER (I-N)

      INCLUDE 'COMMON.F'

      DIMENSION P(NPOIN)
```

```
      PE=(C1*P(I)+C2*P(I+1)+C3*P(I+2))/(30.D0*EL)

      RETURN
      END

*************************************************************

      DOUBLE PRECISION FUNCTION QE(C1,C2,C3,I,EL,Q)

      IMPLICIT DOUBLE PRECISION (A-H,O-Z)
      IMPLICIT INTEGER (I-N)

      INCLUDE 'COMMON.F'

      DIMENSION Q(NPOIN)

      QE=(C1*Q(I)+C2*Q(I+1)+C3*Q(I+2))*EL/420.D0

      RETURN
      END

*************************************************************

      DOUBLE PRECISION FUNCTION FE(C1,C2,C3,I,EL,F)

      IMPLICIT DOUBLE PRECISION (A-H,O-Z)
      IMPLICIT INTEGER (I-N)

      INCLUDE 'COMMON.F'

      DIMENSION F(NPOIN)


      FE=EL/30.D0*(C1*F(I)+C2*F(I+1)+C3*F(I+2))

      RETURN
      END

*************************************************************************
******

      SUBROUTINE INDEX(IELEM)

      IMPLICIT DOUBLE PRECISION (A-H,O-Z)
      IMPLICIT INTEGER (I-N)

      INCLUDE 'COMMON.F'

      INDOF(1) = LNODE(IELEM, 1)
      INDOF(2) = LNODE(IELEM, 2)
      INDOF(3) = LNODE(IELEM, 3)

      RETURN
      END
```

```
************************************************************************
******

      SUBROUTINE ASSEMBLES

      IMPLICIT DOUBLE PRECISION (A-H,O-Z)
      IMPLICIT INTEGER (I-N)

      INCLUDE 'COMMON.F'

      DO 20 J = 1,3
         DO 10 M = 1,3
            JS = INDOF(J)
            KS = INDOF(M)

*
*     ASSEMBLE THE STIFFNESS MATRIX
*
            STIFF(JS,KS)=SMR(J,M)+STIFF(JS,KS)
          STR(JS,KS)=SRR(J,M)+STR(JS,KS)

*             IF (IWRITE .EQ. 2 ) WRITE(40,900) J,K,JS,KS
  900       FORMAT(10X,'ASSEMBLING SMR(',I2,',',I2,') TO STIFF(',I2,
     &      ',',I2,')')
*
   10    CONTINUE
   20 CONTINUE

      RETURN
      END

******************************************************

      SUBROUTINE ASSEMBLEL

      IMPLICIT DOUBLE PRECISION (A-H,O-Z), INTEGER (I-N)

      INCLUDE 'COMMON.F'

*
*     ASSEMBLE THE GLOBAL LOAD VECTOR
*
      DO 70 J=1,3
        JS=INDOF(J)
        RLOAD(JS)=RLOAD(JS)+FLOAD(J)
 70   CONTINUE

      RETURN
      END

************************************************************************
******

      SUBROUTINE BOUNDS

      IMPLICIT DOUBLE PRECISION (A-H,O-Z)
```

```
      IMPLICIT INTEGER (I-N)

      INCLUDE 'COMMON.F'

      BIG  = 1.0D15
      DIAGMAX = 0.0D0

*  SCAN DIAGONAL FOR THE LARGEST ENTRY

      DO 100 N = 1, NPOIN
         IF ( STIFF(N,N) .GE. DIAGMAX ) DIAGMAX = STIFF(N,N)
  100 CONTINUE

      BIG = BIG * DIAGMAX
      IF (NA.EQ.1) THEN
*        RLOAD(1)=RLOAD(1)+AA
        STIFF(1,1)=STIFF(1,1)+ALPHA
      ELSEIF (NA.EQ.2) THEN
        STIFF(1,1)=STIFF(1,1)*BIG
*        RLOAD(1)=UA*STIFF(1,1)
      ELSE
        PRINT*,'ERROR IN NA'
        STOP
      ENDIF
      IF (NB.EQ.1) THEN
*        RLOAD(NPOIN)=RLOAD(NPOIN)+BB
        STIFF(NPOIN,NPOIN)=STIFF(NPOIN,NPOIN)+BETA
      ELSEIF (NB.EQ.2) THEN
        STIFF(NPOIN,NPOIN)=STIFF(NPOIN,NPOIN)*BIG
*        RLOAD(NPOIN)=UB*STIFF(NPOIN,NPOIN)
      ELSE
        PRINT*,'ERROR IN NB'
        STOP
      ENDIF
      RETURN
      END

*******************************************************

      SUBROUTINE BOUNDL
      IMPLICIT DOUBLE PRECISION (A-H,O-Z)
      IMPLICIT INTEGER (I-N)

      INCLUDE 'COMMON.F'

      UB=TMEAN-TFLUC*DSIN(PI/43200.D0*T)
      IF (NA.EQ.1) THEN
        RLOAD(1)=RLOAD(1)+AA
*        STIFF(1,1)=STIFF(1,1)+ALPHA
      ELSEIF (NA.EQ.2) THEN
*        STIFF(1,1)=STIFF(1,1)*BIG
        RLOAD(1)=UA*STIFF(1,1)
      ELSE
        PRINT*,'ERROR IN NA'
        STOP
      ENDIF
```

```
      IF (NB.EQ.1) THEN
        RLOAD(NPOIN)=RLOAD(NPOIN)+BB
*        STIFF(NPOIN,NPOIN)=STIFF(NPOIN,NPOIN)+BETA
      ELSEIF (NB.EQ.2) THEN
*       STIFF(NPOIN,NPOIN)=STIFF(NPOIN,NPOIN)*BIG
        RLOAD(NPOIN)=UB*STIFF(NPOIN,NPOIN)
      ELSE
        PRINT*,'ERROR IN NB'
        STOP
      ENDIF

      RETURN
      END


******************  SUBROUTINE LUDCMP  ****************************
*C
*C     SUBROUTINE LUDCMP
*C
*C---- GIVEN AN NXN MATRIX A, WITH DIMENSION A(NP,NP) THIS
*C     SUBROUTINE FACTORS A INTO AN L*U DECOMPOSITION
*C
*C     REFERENCE: NUMERICAL RECIPES, 1990.
*C
*C     USAGE:
*C     A      GLOBAL STIFFNESS MATRIX ON INPUT
*C
*C            ON OUTPUT, L AND U OVERWRITE THE COEFFICIENTS OF A.
*C
**********************************************************************
********
      SUBROUTINE LUDCMP (A, VV, INDX, N, D)
      IMPLICIT DOUBLE PRECISION (A-H,O-Z),INTEGER(I-N)
      PARAMETER (TINY = 1.0E-20)
      DIMENSION A(N, N), INDX(N), VV(N)
************************************
*c     debug material
*c     ESCHK = 1
*c     IF(ESCHK.NE.1) GO TO 200
*c     WRITE(7,1000) ((a(I,J),J=1,n),I=1,n)
*c1000 FORMAT(/,5X,'[GSTIF] MATRIX :',//,
*c    1      52(1X,52(E8.2,1X),/))
*c 200 CONTINUE
*****************************************
      D = 1.
      DO 20 I = 1, N
        AAMAX = 0.
        DO 10 J = 1, N
          IF (ABS(A(I,J)) .GT. AAMAX) AAMAX = ABS(A(I,J))
   10   CONTINUE
        IF (AAMAX .EQ. 0.) PAUSE 'SINGULAR MATRIX.'
        VV(I) = 1. / AAMAX
   20 CONTINUE
      DO 100 J = 1, N
        DO 40 I = 1, J-1
          SUM = A(I,J)
```

```
        DO 30 K = 1, I-1
          SUM = SUM - A(I,K) * A(K,J)
30      CONTINUE
        A(I,J) = SUM
40    CONTINUE
      AAMAX = 0.
      DO 60 I = J, N
        SUM = A(I,J)
        DO 50 K = 1, J-1
          SUM = SUM - A(I,K) * A(K,J)
50      CONTINUE
        A(I,J) = SUM
        DUM = VV(I) * ABS(SUM)
        IF (DUM .GE. AAMAX) THEN
          IMAX = I
          AAMAX = DUM
        ENDIF
60    CONTINUE
      IF (J .NE. IMAX) THEN
        DO 70 K = 1, N
          DUM = A(IMAX,K)
          A(IMAX,K) = A(J,K)
          A(J,K) = DUM
70      CONTINUE
        D = -D
        VV(IMAX) = VV(J)
      ENDIF
      INDX(J) = IMAX
      IF (A(J,J) .EQ. 0.) A(J,J) = TINY
      IF (J. NE. N) THEN
        DUM = 1./A(J,J)
        DO 80 I = J+1, N
          A(I,J) = A(I,J) * DUM
80      CONTINUE
      ENDIF
100 CONTINUE
    RETURN
    END
******************** SUBROUTINE LUBKSB
*************************************
*C
*C     SUBROUTINE LUBKSB
*C
*C     THIS SUBROUTINE SOLVES THE SET OF EQUATIONS A*X=B.  HERE A IS
INPUT AS
*C     ITS LU DECOMPOSITION DETERMINED BY THE ROUTINE LUDCMP.  INDX IS
INPUT
*C     AS THE PERMUTATION VECTOR RETURNED BY LUDCMP.  B IS INPUT AS THE
LOAD
*C     VECTOR AND RETURNS THE SOLUTION VECTOR, X.
*C
*C     REFERENCE: NUMERICAL RECIPES, 1990.
*C
**********************************************************************
******
      SUBROUTINE LUBKSB (A, INDX, N, B)
```

```
      IMPLICIT DOUBLE PRECISION (A-H,O-Z),INTEGER(I-N)
      DIMENSION A(N, N), INDX(N), B(N)
      II = 0
      DO 20 I = 1, N
        LL = INDX(I)
        SUM = B(LL)
        B(LL) = B(I)
        IF(II .NE. 0) THEN
        DO 10 J = II, I-1
            SUM = SUM - A(I,J) * B(J)
10      CONTINUE
        ELSE IF (SUM .NE. 0.) THEN
          II = I
        ENDIF
        B(I) = SUM
20    CONTINUE
      DO 50 I = N, 1, -1
        SUM = B(I)
        DO 40 J = I+1, N
          SUM = SUM - A(I,J) * B(J)
40      CONTINUE
        B(I) = SUM / A(I,I)
50    CONTINUE
      RETURN
      END


*
*   FILENAME:  COMMON.F
*
       PARAMETER (CVA=719.6D0,CVI=2031.D0)
       PARAMETER (GI=917.D0,GA=1.3D0,TMEAN=-20.D0,TFLUC=0.D0)
       PARAMETER (PI=3.141592654D0,NELEM=25,NPOIN=51)

      COMMON/BND/ AA,ALPHA,BB,BETA,NA,NB,UA,UB
      COMMON/C4/ LNODE(NELEM,3),RLOAD(NPOIN),STIFF(NPOIN,NPOIN),
     &           STR(NPOIN,NPOIN)
      COMMON/C5/ X(NPOIN),DX
      COMMON/C6/INDOF(3)
      COMMON/C7/FLOAD(3),SMR(3,3),SK(3,3),SM(3,3),SRR(3,3)
      COMMON/VARO/TEMPO(NPOIN),CHATO(NPOIN),PHIIO(NPOIN)
      COMMON/VAR/TEMP(NPOIN),PHII(NPOIN),CHAT(NPOIN),VJ(NPOIN)
      COMMON/VARP/TEMPP(NPOIN)
      COMMON/MESH/IWRITE
      COMMON/TIME/H,TMAX,TOUT,T
      COMMON/BLAST/BIG
      COMMON/ERROR/TOL
      COMMON/COUNT/K,KMAX,ITMAX
      COMMON/SLOPE/DTDX(NPOIN)
```